Inflammopharmacology (2023) 31:823–844
https://doi.org/10.1007/s10787-022-01133-5

Inflammopharmacology

ORIGINAL ARTICLE

Anti-inflammatory and antioxidant activities of *Gymnema Sylvestre* extract rescue acute respiratory distress syndrome in rats via modulating the NF-κB/MAPK pathway

Aruna Jangam[1,2] · Satya Krishna Tirunavalli[1,2] · Bala Manikantha Adimoolam[1,2] · Bhavana Kasireddy[1] · Samata Sai Patnaik[1] · Jayashankar Erukkambattu[3] · Jagadeshwar Reddy Thota[1,2,4] · Sai Balaji Andugulapati[1,2] · Anthony Addlagatta[1,2]

Received: 9 July 2022 / Accepted: 30 December 2022 / Published online: 20 January 2023

Abstract

Acute respiratory distress syndrome (ARDS) is one of the major causes of mortality in COVID-19 patients, due to limited therapeutic options. This prompted us to explore natural sources to mitigate this condition. *Gymnema Sylvestre* (GS) is an ancient medicinal plant known to have various therapeutic effects. This investigation examined the therapeutic effect of hydroalcoholic extract of *Gymnema Sylvestre* (HAEGS) against lipopolysaccharide (LPS)-induced lung injury and ARDS in in vitro and in vivo models. UHPLC–HRMS/GC–MS was employed for characterizing the HAEGS and identified several active derivatives including gymnemic acid, gymnemasaponins, gymnemoside, gymnemasin, quercetin, and long fatty acids. Gene expression by RT-qPCR and DCFDA analysis by flow cytometry revealed that several inflammatory cytokine/chemokine, cell injury markers, and reactive oxygen species (ROS) levels were highly upregulated in LPS control and were significantly reduced upon HAEGS treatment. Consistent with the in vitro studies, we found that in LPS-induced ARDS model, pre-treatment with HAEGS significantly suppressed the LPS-induced elevation of inflammatory cell infiltrations, cytokine/chemokine marker expression, ROS levels, and lung injury in a dose-dependent manner. Further mechanistic studies demonstrated that HAEGS suppressed oxidative stress by modulating the NRF2 pathway and ameliorated the ARDS through the NF-κB/MAPK signalling pathway. Additional fractionation results revealed that fraction 6 which has the exclusive composition of gymnemic acid derivatives showed better anti-inflammatory effects (inhibition of IL-6 and IL-1β) at lower concentrations compared to HAEGS. Overall, HAEGS significantly mitigated LPS-induced lung injury and ARDS by targeting the NF-κB/MAPK signalling pathway. Thus, our work unravels the protective role of HAEGS for the first time in managing ARDS.

Keywords Acute respiratory distress syndrome · Cytokine storm · Lung injury · Phytochemicals · *Gymnema Sylvestre* · Gymnemic acid · Neutrophil elastase

✉ Sai Balaji Andugulapati
balaji@iict.res.in

✉ Anthony Addlagatta
anthony@iict.res.in

[1] Department of Applied Biology, CSIR-Indian Institute of Chemical Technology, Hyderabad, Telangana 500007, India

[2] Academy of Scientific and Innovative Research (AcSIR), Ghaziabad, Uttar Pradesh 201002, India

[3] Department of Pathology and Laboratory Medicine, All India Institute of Medical Sciences, Bhopal, Madhya Pradesh 462020, India

[4] Department of Analytical and Structural Chemistry, CSIR-Indian Institute of Chemical Technology, Hyderabad, India

Abbreviations

ARDS	Acute respiratory distress syndrome
BALF	Bronchoalveolar lavage fluid (BALF)
COVID-19	Coronavirus diseases 2019
CRS	Cytokine release syndrome
Dexa	Dexamethasone
ERK	Extracellular signal-regulated kinase
GC–MS	Gas chromatography–mass spectroscopy
GS	*Gymnema Sylvestre*
HAEGS	Hydroalcoholic extract of *Gymnema Sylvestre*
JNK	C-Jun N-terminal kinase
hr	Hour
LPS	Lipopolysaccharide
MPO	Myeloperoxidase
NE	Neutrophil elastase
PBS	Phosphate buffer saline
ROS	Reactive oxygen species
RT-qPCR	Reverse transcriptase quantitative PCR
SRB	Sulforhodamine-B
UHPLC–MS and MS/MS	Ultra performance liquid chromatography–mass spectrometry and tandem mass spectrometry

Introduction

Inflammation-mediated lung diseases are a major cause of morbidity/mortality in COVID-19 patients admitted to intensive care units (Merad and Martin 2020). Pathogenic infections induce hyperactivation of immune cells, leading to cytokine release syndrome (CRS), which is a hallmark of ARDS. Cytokine storm is the main cause of death in COVID-19 patients (Spagnolo et al. 2020). To the best of our knowledge, there is no specific drug to treat ARDS except for a few antibodies that target specific cytokines. The available data are inadequate to conclude the therapeutic effect of IL-6 antibodies (tocilizumab) in the ARDS (Khiali et al. 2020). Cytokines are small secreted proteins produced by nearly every cell to regulate and influence the immune response (Takeuchi and Akira 2010). IL-6 and other pro-inflammatory cytokines (TNFα, IFNγ, IL-10, IL-1β, IL-12p40, IL-17A, IL-2, MIP1α, and IL-8) involve the inflammatory cascade and contribute to host defence against infections. Inflammatory chemokines such as CCL-2, CCL-7, and CXCL-1 act as a chemoattractant for leukocytes, recruiting monocytes, neutrophils, and other effector cells and initiating the infiltration of inflammatory cells from the blood to sites of infection or the target organ. In addition to inflammatory cells, respiratory epithelium or lung epithelial cells are also involved in maintaining the integrity of the lungs, their function, and host responses to pathogenesis and resolution of ALI/ARDS upon infections (Manicone 2009). The pathogenesis of ALI/ARDS is significantly influenced by excessive oxidative stress and inflammation (Proudfoot et al. 2011). The activation of the nuclear factor erythroid 2-related factor 2 (Nrf2) pathway is one of the primary defence mechanisms against oxidative stress-induced injury to cells (Ci et al. 2017). Upon induction of oxidative stress, NRF2 translocates into the nucleus, binds to downstream antioxidant response elements, and stimulates the transcription of antioxidant genes such as heme oxygenase-1 (HO-1), superoxide dismutase (SOD), NAD(P)H-quinone oxidoreductase 1 (NQO1), and catalase to initiate the defence mechanism (Baird and Yamamoto 2020).

Despite the advances in ventilator and intensive care therapies with novel drugs, the mortality rate remains high and exceeds 50% in ARDS patients (Aslan et al. 2021). Due to the lack of first-line treatment for ARDS, glucocorticoids are being used as an anti-inflammatory and immunosuppressive agent and their outcomes have not been proven to be beneficial (Barnes and Adcock 1993). Therefore, identifying safe and efficacious compounds which target the pro-inflammatory, inflammatory and oxidative stress markers/indicators are highly warranted to mitigate the ARDS-induced cytokine storm and improve the treatment outcome.

Gymnema Sylvestre (GS), is a phytopharmaceutical used in Ayurveda to treat diabetes and various inflammatory diseases (Tiwari et al. 2014a; Baskaran et al. 1990). GS belongs to the Asclepiadaceae family and is found in tropical forests of India, Africa and Australia (Kanetkar et al. 2007a). The main constituents of GS include gymnemic acids, which are triterpenoid saponins responsible for antidiabetic activity (Leach 2007). In addition to gymnemic acids, GS contains alkaloids, anthraquinones, chlorophylls, flavones, quercitol, etc., that mitigate the inflammatory markers. An extract of GS significantly reduced the paw oedema volume by 48% and inhibited granuloma formation at 300 mg/kg compared with the control group (Malik et al. 2008). Ethanol extract of GS is known to reduce blood sugar and lipid levels in various animal models (Tiwari et al. 2014b). The blood glucose-lowering effects of GS extract are due to the inhibition of T1R2 + T1R3 sweet receptors by gymnemic acid and its derivatives, thereby reducing glucose absorption (Kanetkar et al. 2007b; Sahu et al. 1996). In a different study, hydroalcoholic extracts also mitigated ulcerative colitis in Wistar albino rats by suppressing the oxidative and inflammatory response and protecting the colonic mucosal content (Aleisa et al. 2014). These beneficial effects were achieved by reducing the level of pro-inflammatory cytokines such

as IL-1β, IL-6 and TNF-α in the colon tissue. Other components such as quercetin also exhibit strong antioxidant and anti-inflammatory activity against various disease models (Li et al. 2016b). It has been established that gymnemic acid alleviates inflammation and insulin resistance in db/db mice via the PPARδ- and NFκB-mediated pathways Li et al. (2019). Recent simulation studies on bioactive molecules of GS revealed that gymnemic acid is a ligand binding with a 3CLpro as a COVID-19 therapeutic target (Subramani et al. 2020). Together, these studies have prompted us to evaluate the protective nature of the hydroalcoholic extract GS (HAEGS) against LPS-induced in vitro and in vivo ARDS models. We further separated various components on column chromatography and identified a specific fraction that mimicked the anti-inflammatory properties of the whole hydroalcoholic extract. Systematic chemical characterization established the chemical composition of the extract. By adopting various biochemical tools, we established the possible mechanism for the therapeutic activity of HAEGS.

Experimental methodology

Materials

Lipopolysaccharide (LPS) from *E. coli* 055: B5, LC–MS and HPLC-grade solvents and fine chemicals were procured from Sigma-Aldrich, USA. SYBR green mix cDNA synthesis kits were purchased from Takara Bioscience, India. ELISA kits (IL-6, CCL2, INF-γ and IL-1β) were obtained from R&D Systems. Primary antibodies were purchased from Cell Signaling Technology, USA, and the corresponding catalogue numbers are mentioned in supplementary table S2. Bicinchoninic acid reagent (BCA kit) was bought from Thermo Scientific, USA. Polyvinylidene difluoride (PVDF) membrane (0.45 µm) was procured from Millipore, USA. Secondary antibodies were procured from Jackson Laboratory, USA, and an ECL kit was purchased from Advansta, Menlo Park, CA, USA. Deionized water (18 MΩ) was used for the preparation of all solutions. Leaves of G. Sylvestre were collected from Chittoor district, Andhra Pradesh, India. The plant specimen was authenticated by a botany professor from Osmania University, Hyderabad, India. LC–MS CHROMASOLVs-grade and HPLC-grade methanol (MeOH) and acetonitrile (ACN) were procured from Sigma-Aldrich (St Louis, USA). Analytical reagent (AR)-grade ammonium acetate, ammonium formate, formic acid, hydrochloric acid (HCl).

Cell lines and culture conditions

RAW-264.7 cell line (murine macrophages) was procured from ATCC and cultured in DMEM (Dulbecco's modified Eagle's) medium with 1.5 g/l sodium bicarbonate, 4 mM L-glutamine, 4.5 g/l glucose, and 10% FBS (fetal bovine serum). The human bronchial epithelial cell line (BEAS-2B cell line) was purchased from Lonza, USA, and cultured using BEGM media with growth factors. Both the cell lines were cultured in a 5% CO_2 incubator with a humidified atmosphere of 95% air at 37 °C. All cell lines were used in between four and five passages.

Preparation of hydroalcoholic extract of *Gymnema Sylvestre* (HAEGS)

The shade-dried leaves of *Gymnema Sylvestre* were powdered and a hydroalcoholic maceration method was employed for extracting the hydroalcoholic GS extract. The coarse powder (639 g) of *Gymnema Sylvestre* was added into the mixture of 5.62 L of ethanol and 1.87 L of water (in a 3:1 ratio) in a beaker with constant stirring using magnetic stirrers for a period of 48 h at 25 °C. The extracted solution was filtered through a muslin cloth and evaporated to dryness using a rotary evaporator at a temperature below 55 °C under a vacuum. The dried powder of HAEGS was stored at 4 °C in coloured glass bottles until further use.

Fractionation of HAEGS

Part of the crude extract (HAEGS) were dissolved in acetone:chloroform solvent mixture and loaded onto a silica column (Fig. S8A). For separating various compounds, a mixture of acetone:hexane (shown in Scheme 1), a mixture of methanol:chloroform in various ratios, and lastly methanol solvents were used. By increasing the polarity, 30 fractions were collected in total, and the fractions with similar thin layer chromatography (TLC) patterns (Fig. S8B) were mixed to afford six major fractions (F1–F6). Fraction 31 (labelled as F7) obtained with methanol elution did not provide any detectable organic molecules and hence it was discarded.

Phytochemical profiling of HAEGS extract

Sample preparation

The samples were dissolved in methanol, centrifuged and filtered using a 0.22 µm membrane filter and the final concentrations of the crude samples were injected (1 µL) into the UHPLC/Thermo Orbitrap Exactive mass spectrometer (Thermo Scientific, Bremen, Germany) system.

Development and optimization of the chromatographic conditions

Analytical separations of HAEGS were achieved on a Surveyor UHPLC system (Thermo Scientific, Germany)

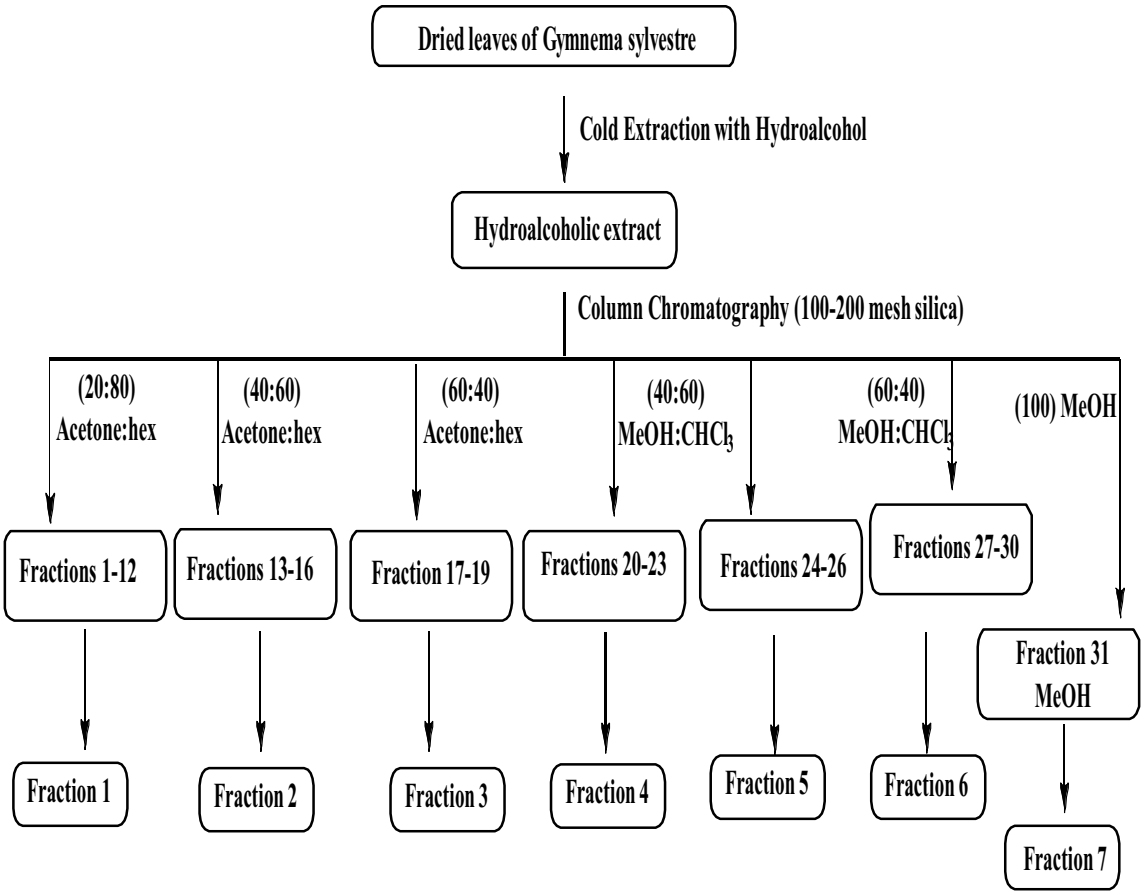

Scheme 1 Schematic representation of the preparation and fractionation of hydroalcoholic extract of *Gymnema Sylvestre*

consisting of a quaternary gradient pump, an auto-injector and an in-line degasser. The column compartment was maintained at a temperature of 25 °C. The chromatographic separation method was developed in reverse phase mode with Syncronis C18 column (2.1 × 100 mm; Thermo Scientific, Germany) (Dadinaboyina et al. 2021). Varying the selectivity determination factors such as pH of mobile phase, ratios of polarity change and flow rate optimized the method. Finally, acceptable separation was achieved using 0.1% formic acid in water (A) and acetonitrile (ACN) (B) with a flow rate of 0.15 mL min^{-1} in gradient elution mode. The following linear gradient elution was used: (time in min/%B): 0–1/5, 1–12/95, 12–16/95, 16–21/5, and 21–26/5. The column was equilibrated with 20 column volumes of mobile phase at the composition before sample injection and the injection volume was 1 µl.

Mass spectrometry

Mass spectral analysis was carried out on Thermo Orbitrap Exactive mass spectrometer (Thermo Scientific, Bremen, Germany). The eluent from the UHPLC system was directed in the mass spectrometer via heated electrospray ionization (HESI) interface and operated in the positive and negative ion modes. The mass spectrometer was calibrated before analysis using the manufacturer's calibration solution (ProteoMass LTQ/FN-Hybrid ESI Pos. Mode Cal Mix, SUPELCO) to obtain the mass range in external calibration mode. Parameters of the ion source were as follows: positive ion spray voltage 3.50 kV, negative ion spray voltage 2.50 kV, heater temperature 275 °C, capillary temperature 320 °C, capillary voltage 67.50 V, tube lens voltage 140 V, skimmer voltage 20 V, sheath gas flow 30 (arbitrary units), auxiliary gas flow 15 (arbitrary units) and sweep gas 0 (arbitrary units). Nitrogen was used as the sheath and auxiliary gas in the ion source. The instrument was operated in full scan and automatic MS/MS experiments over the range of 100–2000 m/z at a resolving power of 100,000 (full width at half maximum) using nitrogen as collision gas.

GC–MS analysis

The GC analysis was performed using Agilent 6890 GC equipped with Agilent Technologies 5977A mass selective

detector (MSD). The separation of analytes was carried out on a capillary column (Agilent) HP-5 5% Phenyl Methyl Siloxane (30m × 250 µm × 0.5 µm). The injection port temperature was maintained at 240 °C and the oven was programmed from 50 to 280 °C at a ramp rate of 10 °C/min with the initial hold-up temperature time as 2 min and the final hold-up temperature time as 5 min. Helium was used as a carrier gas at a flow rate of 1.2 mL/min. The desorption of analytes and injection into the column was carried out in splitless mode to avoid the loss of low abundant volatiles. GC–MS interface, ion source and quadrupole temperatures were maintained at 280 °C, 230 °C, and 150 °C respectively. The ionization of volatiles was carried out in an electron ionization source at 70 eV electron energy, and the scan range was fixed at 30–800 units. The volatile organic compounds were identified by using the W9N11.L, NIST14 library database. Mass spectral data were processed using MSD Chem Station.

In-vitro assays

Treatment conditions for in vitro experiments

Macrophage (RAW-264.7) cells were seeded in 24-well plates (0.5×10^5/well) for estimating the IL-6 levels using ELISA. For all other cell culture experiments, RAW-264.7 or BEAS-2B cells were seeded in six-well plates (3×10^5/well) and incubated for 18 h, then cells were washed with phosphate buffer saline (1xPBS) and cultured with serum-free media for another 6 h. Further, cells were pre-treated with HAEGS (125, 250 and 500 µg/mL), different fractions of indomethacin (50 and 100 µM) or dexamethasone (100 and 500 ng/mL) for 2 h, then activated with LPS (1 µg/mL for RAW-264.7 and 5 µg/mL for BEAS-2B cells) and incubated for 12 h. Then, cell supernatant was collected for nitric oxide estimation and ELISA, while cells were harvested for gene expression and Western blot analysis.

Cell viability by SRB assay

Sulforhodamine-B (SRB) assay was performed for assessing the cell viability as published previously (Tirunavalli et al. 2021a). Briefly, 5×10^3 cells/well were seeded in a 96-well plate and then treated with sterile water (vehicle control) or HAEGS at various concentrations (125, 250 and 500 µg/mL) in the presence or absence of LPS. After 48 h, an SRB assay was performed. IC_{50} values were calculated using the curve-fit method by GraphPad Prism-5.

Gene expression analysis

After the treatment period, treated cells or rat lung tissues were subjected to RNA isolation using RNAiso plus as described earlier (Andugulapati et al. 2020). Briefly, RNA was isolated using the TRIzol–chloroform method and total RNA was quantified using nano-drop. Isolated RNA (1 µg) was subjected to cDNA synthesis using a prime script cDNA synthesis kit as per the manufacturer's instructions. Specified primers [*IL-6, IL-1β, TNF-α, IL-8, CCL2, CCL3, CCL7, CXCL1*, alveolar pulmonary stretch (amphiregulin), *CC16*, vascular cell adhesion molecule-1 (*VCAM-1*), intercellular adhesion molecule *(ICAM-1)*, and reference markers *(GAPDH, β2M, and β-actin*)] were designed using Primer-3 software and the respective sequences are shown in Table S1. RT-qPCR was carried out using SYBR green mix and the differences in mRNA expression of the specified genes were calculated as the fold change using the formula $2\text{-}^{\Delta\Delta ct}$ and data were expressed as mean ± SEM.

ROS measurement using the DCFDA assay

ROS estimation was performed using DCFDA staining as described earlier (Tirunavalli et al. 2021b). Briefly, after pre-treating the cells with specified concentrations of HAEGS for 2 h, cells were activated with LPS for another 12 h. Then DCFDA assay was performed using BD-Accuri® C6 flow cytometer for mean fluorescence intensity of DFCDA.

Immunoblotting analysis

Cells or rat lung tissues that were treated by HAEGS followed by LPS stimulation were subjected to Western blot analysis as described earlier (Andugulapati et al. 2020). Briefly, cells or tissue samples were lysed using RIPA lysis buffer and then protein concentrations were estimated using a BCA kit. Then, 30 µg of protein per sample was loaded onto the SDS-PAGE Bis–Tris 8–12% protein gel for electrophoresis and then transferred onto PVDF membranes. Further, the PVDF membrane was blocked with 5% BSA (Sigma Aldrich, USA) for 1 h at room temperature, followed by incubation with primary antibodies overnight at 4 °C. Then the respective secondary antibodies were added and then blots were developed using an ECL kit.

In vivo experiments

Induction of ARDS using intratracheal instillation of LPS

Adult SD (male) rats weighing 210–240 g, ($n = 32$) were used for developing the LPS-induced ARDS. As per the Committee for the Purpose of Control and Supervision on Experiments on Animals (CPCSEA) regulations, all the animals were acclimatized at a specified temperature (24–26 °C) with the maintenance of 12 h dark and 12 h light cycles. The experimental protocol was approved by Institutional Animal Ethics Committee (IAEC) (IICT/023/2020),

CSIR-Indian Institute of Chemical Technology 6). Male SD rats were randomly assigned to four groups ($n = 8$/group). Before LPS administration, rats were pre-treated with HAEGS 125 mg/kg and 250 mg/kg in group 3 and group 4 of the animals, respectively. LPS was dissolved in PBS to attain a concentration of 5 mg/mL. All animals were anaesthetized with ketamine (80 mg/kg) and xylazine (10 mg/kg). After 12 h of the pre-treatment, rats were challenged with LPS (5 mg/kg) intratracheally, in treatment groups (groups 3 and 4) and the LPS control group (group 2). Group 1 of rats were used as a sham control, where PBS was instilled into the rat's trachea, while the remaining three groups were used to establish the ARDS model. After 12 h of LPS administration, rats were again dosed with HAEGS and monitored for a further 12 h. After 24 h of the LPS stimulation, Bronchoalveolar lavage Fluid (BALF) samples were collected from 50% of the animals from each group and one part of the BALF samples were subjected to neutrophil count and, remaining BALF sample was centrifuged and stored at − 80° in a freezer for ELISA. All animals were killed and the left lungs were isolated and collected in buffered formalin and subjected to histopathological examination, while the two lobes of the right lungs were collected for wet-to-dry (W/D) analysis and the remaining two lobes were collected for Western blotting, reverse transcription-quantitative PCR (RT-qPCR), ELISA and nitric oxide examinations.

Lung wet–dry weight (W/D) ratio

After killing the animals, one of the right lung tissues was isolated and rinsed with 1XPBS, then the surface liquid of the lobe was removed by draining with clean filter paper, and the wet weight was recorded. Then these lung tissues were incubated in a thermostatic oven at a constant 80 °C for 48 h, followed by measuring the dry weight. The W/D ratio was estimated to measure the moisture content in the lung tissues.

BALF analysis

Animals were anaesthetized with pentobarbital 50 mg/kg and then BALF was collected after exposing the trachea. Then the trachea was cannulated, and a volume of 3 ml sterile saline was slowly infused into the lungs and 2 mL of BALF collected. BALF cell pellet was collected by centrifuging the BALF at 1800 rpm at 4 °C for 12 min, and the cell pellet was re-suspended in 500 µL of sterile saline to quantify inflammatory cell counts using a cell counter.

Estimation of IL-6 CCL2 and IL-1β using ELISA

IL-6, CCL-2 and IL-1β protein levels were measured in cell culture supernatants, BALF and lung tissue homogenates using ELISA kits (R&D Biosystems, Minneapolis, MN, USA) as per the manufacturer's instructions.

Nitric oxide estimation

Nitric oxide estimation was performed as described in our earlier publication (Tirunavalli et al. 2021a). Briefly, cell supernatant (cell culture or tissue homogenates) was collected and used to estimate the NO levels. Griess reagent was used to evaluate the NO levels of the samples by mixing both supernatants of the lung tissue samples and Griess reagent (1:1 ratio). The reaction mix was incubated at 37 °C for 10 min in dark conditions, and absorbance was measured at 548 nm.

Histopathology and immunohistochemistry

Histopathology and immunohistochemistry were performed as described earlier (Tirunavalli et al. 2021a). Briefly, a part of the pulmonary lobe was isolated, rinsed with ice-cold PBS, and fixed with 10% neutral-buffered formalin. Paraffin blocks were prepared and sectioned (4 µm), followed by staining with haematoxylin and eosin (H&E) and periodic acid–Schiff (PAS) staining. A few sections were taken on positively charged (Thermo Fisher, USA) slides for immunohistochemistry analysis. The pathological changes in the lungs and alveolitis in lung tissues were scored and semi-quantitatively assessed by a pathologist using H&E staining. The scoring system of pathological changes was: 0, no pathologic changes; 1, patchy changes; 2, local changes; 3, scattered changes; 4, severe changes (in most parts of the lung) (Alavinezhad et al. 2017). Immunohistochemistry was performed as described in the previous protocol (Tirunavalli et al. 2021a). Briefly, tissue sections were incubated with primary antibodies for 16 h. Sections were washed and stained with secondary antibodies. The protein expression was detected using SignalStain® DAB Chromogen Kit. Neutrophil elastase, MPO, NRF2 and HO-1protein (Immunohistochemistry) relative expressions were quantified using Image J software and plotted as graphs for a better representation of the results.

Statistical analysis

All experimental results were expressed as mean ± standard error of the mean (SEM) and analysed with the GraphPad Prism 5.0 software. All data were analysed by one-way or two-way ANOVA with multiple comparisons, where appropriate. In all cases, $P < 0.05$ was considered statistically significant.

Results

Characterization of HAEGS

Hydroalcoholic extract of *Gymnema Sylvestre* was analysed by LC–ESI-HRMS and MS/MS under both positive and negative ion modes. The resulting mass spectra showed intense $[M+H^+$ and $[M-H]^-$ ions corresponding to the plant secondary metabolites in positive and negative ion modes, respectively (Tables S3–S6). MS data showed possible elemental compositions with mass accuracy of less than ± 4.5 **Δ** ppm error. These ions were subjected to MS/MS analysis for further characterization. The resulting MS and MS/MS data were processed through the compound discoverer (version 3.2) using a database (Workflow Templates/LC/Natural Product/Natural Product Unknown ID w stats online and Local Database Searches, Reaxys and DNP) and identified a total of 112 metabolites and the majority of these metabolites were derivatives of gymnemic acid, gymnemasaponins, gymnemoside, gymnemasin, and quercetin (Table S3 and S4). In addition, 20 gymnemic acid analogues and 10 flavonoids were manually identified by accurate mass spectral data and are presented in Fig. 1A, Figs. S1–S3, Tables S5 and S6. Similarly, the methanolic extract of HAEGS was analysed using GC–MS and identified a total of 35 secondary metabolites (Fig. 1B, and Table S7), which include 12 fatty acids (stearic acid, palmitic acid, linolenic acid, octadecenoic acid, stearin, squalene, g-tocopherol), cholesterol, and vitamin E (Fig. 1B, and Table S7). The identified metabolites were corroborated with the database analysed (for this identification, W9N11.L and NIST14 library databases were used). Overall, our analysis showed that HAEGS is a mixture of several active phyto-molecules.

HAEGS attenuated the LPS-induced cytokine levels in mouse macrophages

Excessive cytokine release is considered to be one of the critical causes of ARDS and multiple-organ failure (Chousterman et al. 2017). SARS-CoV-2-induced ARDS exhibited elevated levels of IL-6 in several patients (Tang et al. 2020b) and it plays a key role in disease progression. Before investigating the effect of HAEGS on IL-6 levels, a cell viability assay was conducted, and the results revealed that HAEGS (125 and 250 µg/mL) treatment showed more than 90% cell viability in the presence or absence of LPS (Table. S8). To determine the effect of HAEGS against LPS-induced IL-6 release, in vitro assays were performed using RAW-264.7 cells and IL-6 estimation was performed using ELISA. Treatment with LPS (1 µg/mL) significantly increased the IL-6 levels compared to vehicle control, and pre-treatment with HAEGS (125, 250, and 500 µg/mL) significantly mitigated LPS-induced IL-6 levels compared to LPS control (Fig. S4 and Table S8). Further, to investigate the effect of HAEGS on cytokines and chemokines, RT-qPCR analysis was performed using RAW-264.7 cells upon LPS stimulation. The RT-qPCR analysis showed that LPS induction significantly increased the cytokine, chemokine, and inflammatory marker's expression compared to vehicle control (Fig. 2A–G). Pre-treatment with HAEGS or dexamethasone (Dexa) reduced the cytokines, chemokines, and inflammatory marker expression in a dose-dependent manner (Fig. 2A–G). Taken together, HAEGS significantly ameliorated the LPS-induced cytokine expression in a dose-dependent manner.

HAEGS mitigated the LPS-induced cytokine levels in lung epithelial cells

ARDS is a disease that is the result of alveolar epithelial cell injury and pulmonary endothelial cell damage with upregulation of several inflammatory cytokines typically called cytokine storm (Bachofen and Weibel 1977). Others and we (Tirunavalli et al. 2021a; Kany et al. 2019) demonstrated that stimulation with LPS (5 µg/mL) significantly increased various cytokines (including IL-6, TNF-α and IL-1β) and lung epithelial cell damage markers in BEAS-2B cells. Similarly, RT-qPCR analysis revealed that LPS stimulation increased the expression of cytokine markers (*IL-6, TNF-α, and IL-1β*) and treatment with HAEGS significantly mitigated the same (Fig. S5A–C). Inflammatory markers such as *COX-2* were also increased in LPS stimulation and treatment, with significant HAEGS attenuation (Fig. S5D). Pro-inflammatory chemokines such as *IL-8, CCL2, CCL7 and CXCL-11* play a major role in inflammation. To investigate whether the HAEGS protects cells from LPS-mediated elevation of chemokines, mRNA expression of various chemokine markers were estimated upon LPS exposure to BEAS-2B cells. mRNA expression analysis revealed that LPS stimulation significantly increased chemokine expression, and pre-treatment with HAEGS reduced the chemokine expression in a dose-dependent manner (Fig. S5E-S5H). HAEGS reduced the chemokine levels better than or equal to dexamethasone. *CC-16* and amphiregulin were reported to be elevated in patients with ventilator-associated lung injury and asthma and also plays a major role in epithelial cell damage along with adhesion molecules (Ogata-Suetsugu et al. 2017; Determann et al. 2009). Further, RT-qPCR analysis was extended to investigate the expression of adhesion molecules and lung epithelial cell damage marker CC-16. Interestingly, HAEGS reduced the LPS-induced *CC-16*, amphiregulin, *VCAM* and *ICAM* marker's expression compared to LPS control

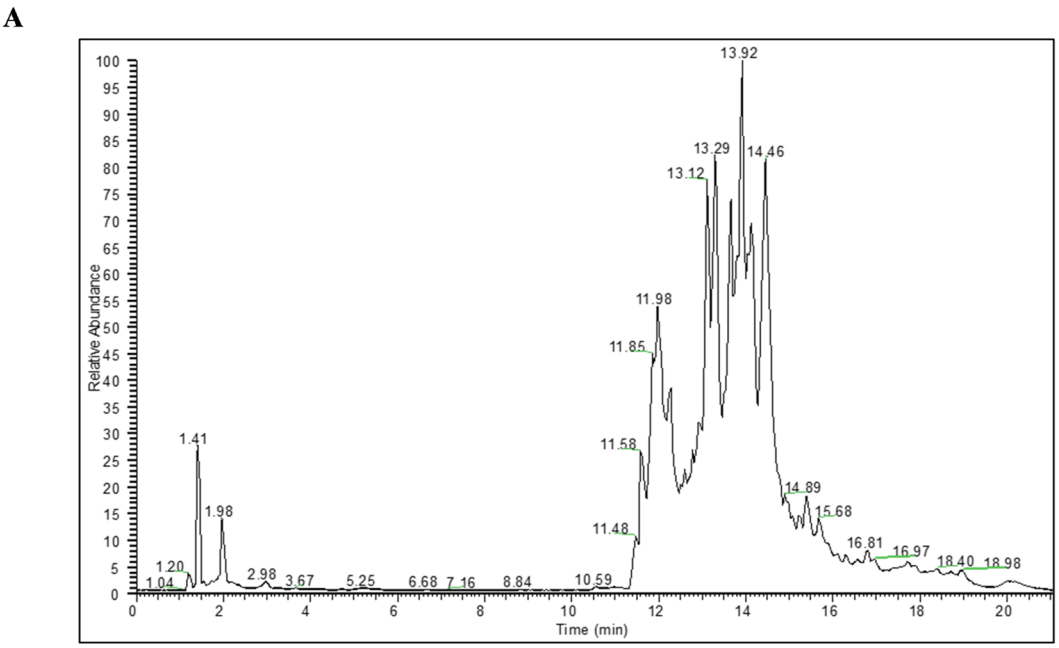

UHPLC-ESI-Orbitrap Total ion chromatogram of HAEGS.

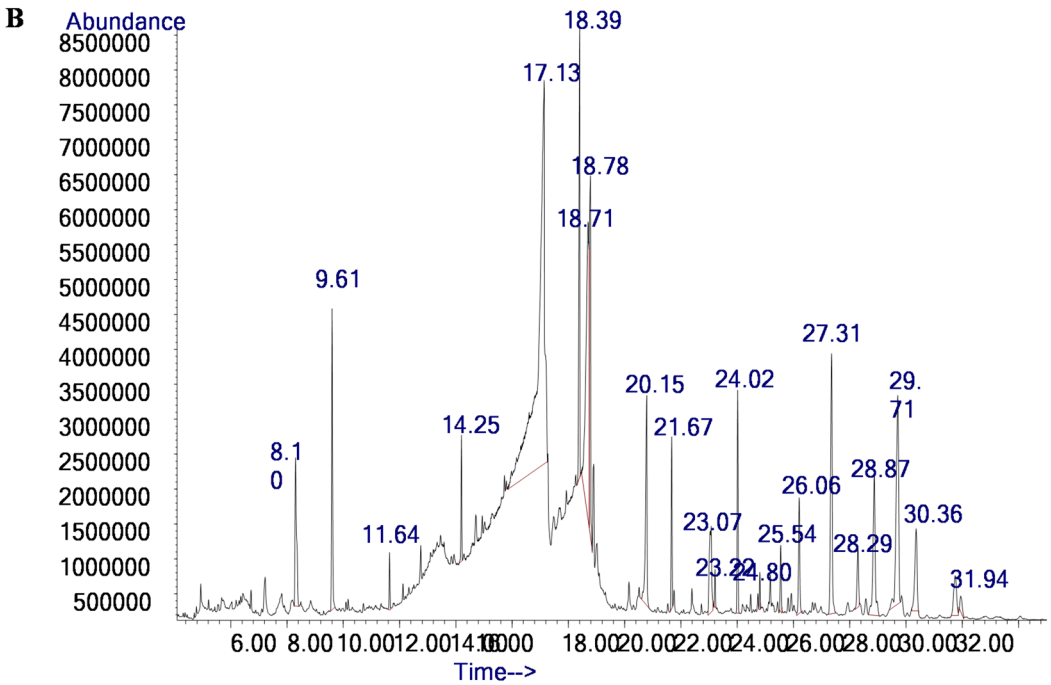

Total ion chromatogram (GC-MS) of HAEGS.

(Fig. 2H–K). Overall, HAEGS pre-treatment significantly mitigated the LPS-induced cytokine, chemokine, and inflammatory markers' expression equivalent to dexamethasone.

LPS-induced ROS levels were abrogated with HAEGS pre-treatment

Reactive oxygen species (ROS) are one of the key signalling molecules that play a substantial role in the

◂**Fig. 1** Chromatographic and GC analysis of HAEGS. **A** Chromatographic separations of *Gymnema Sylvestre* plant extract was carried out on a Surveyor UHPLC system using a Syncronis C18 column (2.1 × 100 mm) with a gradient mobile phase of acetonitrile and 0.1% formic acid in water with a flow rate of 0.15 mL/min. In the LC–HRMS analysis, a total of 20 plant secondary metabolites were identified based on the derived elemental compositions from the high-resolution mass spectral data. Thermo Xcalibur software (version 2.2) was used for processing the mass spectral data. **B** The GC analysis was performed with Agilent 6890 GC equipped with Agilent Technologies5977A mass selective detector (MSD). The separation of analytes was carried out on capillary column (Agilent) HP-5% Phenyl Methyl Siloxane (30 m × 250 um × 0.5 um). The volatile organic compounds were identified by using the W9N11.L, NIST14 library database. In this analysis, a total of 19 plant secondary metabolites were identified. Mass spectral data were processed using MSD ChemStation

progression and maintenance of inflammatory disorders. LPS induces the expression of ROS through multiple mechanisms including the suppression of antioxidant enzymes and induction of NADPH oxidase involved in the ROS production (Li et al. 2010). To study whether HAEGS pre-treatment reduces the levels of NO and ROS levels, we performed nitric oxide estimation and DCFDA measurement assays. Nitric oxide analysis revealed that LPS significantly increased the NO levels in LPS control, and pre-treatment with HAEGS significantly reduced the NO levels in mouse macrophages (Fig. S6A). Similar to the NO assay, the DCFDA assay revealed that LPS increased the ROS levels in LPS control and treatment with HAEGS or Dexa reduced the ROS levels in a dose-dependent manner (Figs. 3A, B and S6B, C).

HAEGS treatment suppressed the cytokine levels by modulating the NF-κB and p38 phosphorylation

Several reports have shown that NF-κB signalling causes the elevated expression of pro-inflammatory genes, including those encoding chemokines and cytokines (Lawrence 2009). Further, to elucidate the mechanism of action of HAEGS, RAW-264.7 or BEAS-2B cells were pre-treated with HAEGS and further stimulated with LPS. After 12 h incubation, cells were subjected to Western blot analysis for elucidation of the mechanism. LPS stimulation increased the phospho-p65 and HAEGS treatment significantly reduced the phospho-p65 levels in a dose-dependent manner in both the cell types (Fig. 3C, D, F and G). MAPK pathway is known to regulate the LPS-mediated inflammation in RAW-264.7 cells. Immunoblotting analysis revealed that LPS stimulation increased the phospho-p38 levels, and with treatment with HAEGS, the same markers were reduced significantly (Fig. 3C and E). Overall, these results demonstrated that HAEGS modulated the NF-κB/MAPK pathway.

Treatment with HAEGS abrogated the infiltration of inflammatory cells and cytokine storm in rat lungs

The cascade of lung inflammation/injury involves various inflammatory responses from various cell types including macrophages, immune cells, endothelial and epithelial cells. Inflammatory cells such as neutrophils, leucocytes or monocytes respond immediately and cause inflammatory cell infiltrations into the affected organs (Turner et al. 2014). In in vivo, several parameters play a major role in inducing ARDS/lung injury. It was reported that oedema occurs as a result of acute lung inflammation, leading to an increase in lung weight. This could be due to increased infiltration of inflammatory cells because of neutrophil-mediated chemotaxis. To investigate the effect of HAEGS against LPS-induced ARDS, a rat model was employed (Fig. S7). After 24 h of the treatment, BALF was collected from rat lungs, then animals were sacrificed, and the lungs were isolated. Lung index analysis showed that LPS alone group showed increased lung weight (wet/dry ratio) compared to sham control, whereas in the treatment group, lung weights were normal, and compared to LPS alone lung weights were significantly reduced (Fig. 4A). Further BALF analysis revealed that neutrophil cell percentage was increased four times in LPS alone group and treatment with HAEGS significantly mitigated the LPS-induced infiltration of neutrophils (Fig. 4B). Further, RT-qPCR analysis revealed that LPS induced several pro-inflammatory cytokines and chemokines in LPS-treated rats compared to sham control lung tissues. Treatment with HAEGS (125 mg/kg and 250 mg/kg) significantly mitigated the cytokine and chemokine levels (Fig 4C–I). These results revealed that pre-treatment with HAEGS significantly ameliorated the LPS-induced inflammatory mediators' response in the lungs.

Treatment with HAEGS mitigated the LPS-induced cytokine levels in BALF samples and in lung tissues

To validate the BALF analysis and gene expression data, BALF samples and lung tissue samples were subjected to ELISA. IL-6 levels were significantly increased in LPS control group samples (BALF and tissue), whereas treatment with HAEGS significantly reduced the IL-6 levels (Fig. 5A and B). Further investigation was extended to estimate CCL-2, and IL-1β using lung tissue samples. ELISA results revealed that HAEGS treatment significantly reduced the LPS-induced elevation of IL-1β and CCL2 levels (Fig. 5C and D). Overall, protein expression data validated the gene expression results and it confirmed the protective action of HAEGS against LPS-induced cytokine expressions.

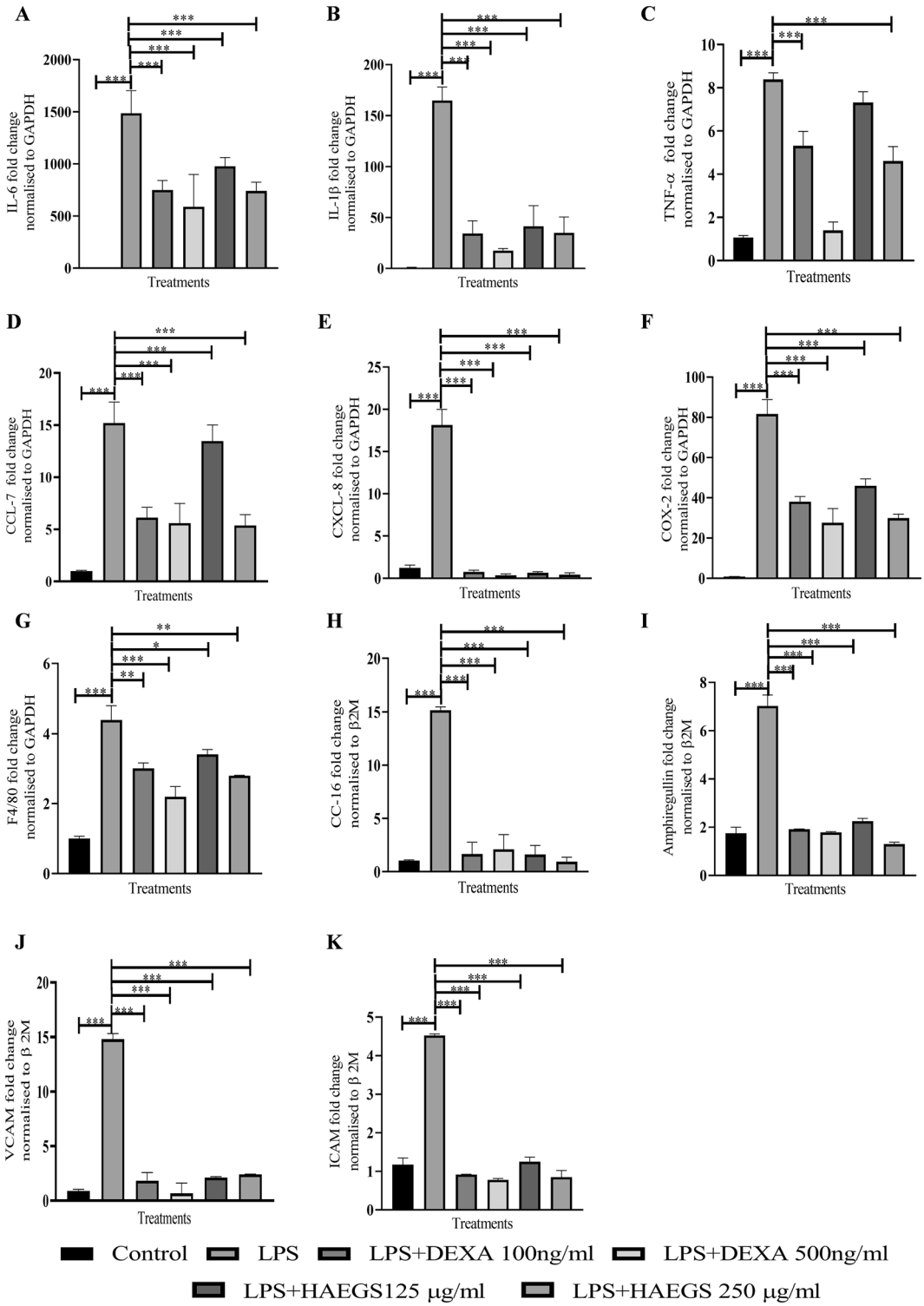

Fig. 2 HAEGS treatment mitigated the LPS-induced pro-inflammatory and chemokine marker's expression in RAW 264.7 and epithelial cells. **A–G** RAW-264.7 cells were cultured in serum-free media for 6 h, then cells were pre-treated with HAEGS (125 and 250 µg/mL) or dexamethasone (100 ng/mL and 500 ng/mL), for a period of 2 h; then cells were stimulated with LPS (1 µg/mL) for a period of 12 h. **H–K** BEAS-2B cells were pre-treated with HAEGS (125 and 250 µg/mL) or DEXA (100 ng/mL and 500 ng/mL) for 2 h; further, cells were stimulated with LPS (5 µg/mL) for another 12 h. Thereafter, cells were subjected to qRT-PCR analysis using specified primer sets. Graphs in panels represent fold change in gene expression normalized to β2M. $*p<0.05$, $**p<0.01$, $***p<0.001$. *NS* non-significant. One-way ANOVA was performed for statistical analysis. Data represented as mean ± SEM, $n=3$

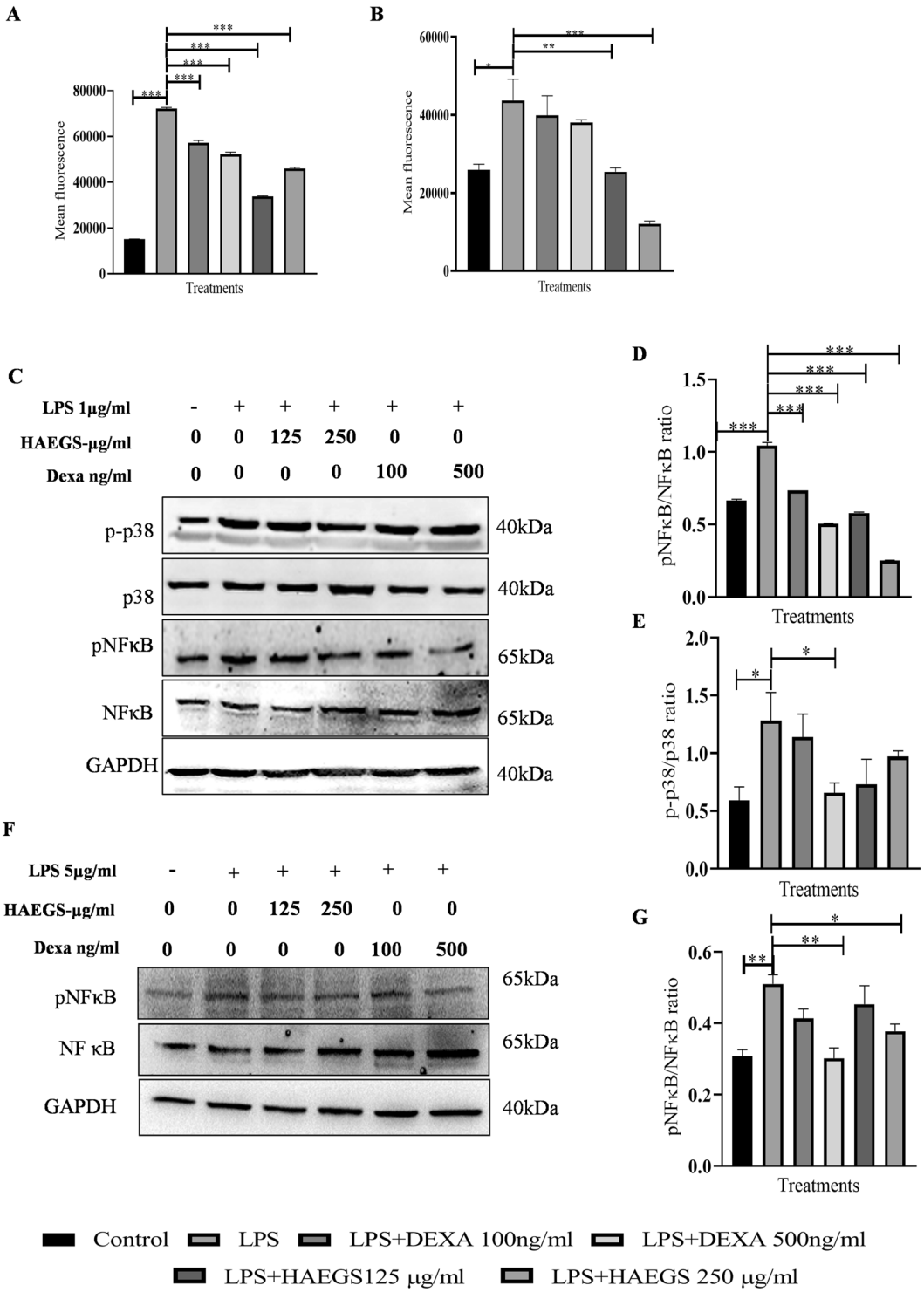

Fig. 3 HAEGS treatment mitigated the oxidative stress by modulating the MAPK and NF-κB pathways. **A**, **B** RAW-264.7 (**A**) or BEAS-2B (**B**) cells were pre-treated with HAEGS (125 and 250 µg/mL) or DEXA (100 ng/mL and 500 ng/mL) for 2 h, then cells were stimulated with LPS (1 µg/mL or 5 µg/mL) or for another 12 h. Thereafter, cells were trypsinized and subjected to DCFDA analysis using flow cytometry. **C–G** RAW-264.7 (**C**–**E**) or BEAS-2B (**F**–**G**) cells were pre-treated with HAEGS (125 and 250 µg/mL) and DEXA (100 ng/mL and 500 ng/mL) after 2 h, and cells were stimulated with LPS (1 µg/mL) for another 12 h. Further, cells were subjected to Western blot analysis using specified antibodies. Protein expressions were quantified using Image J software and graphs were plotted against each specified protein marker

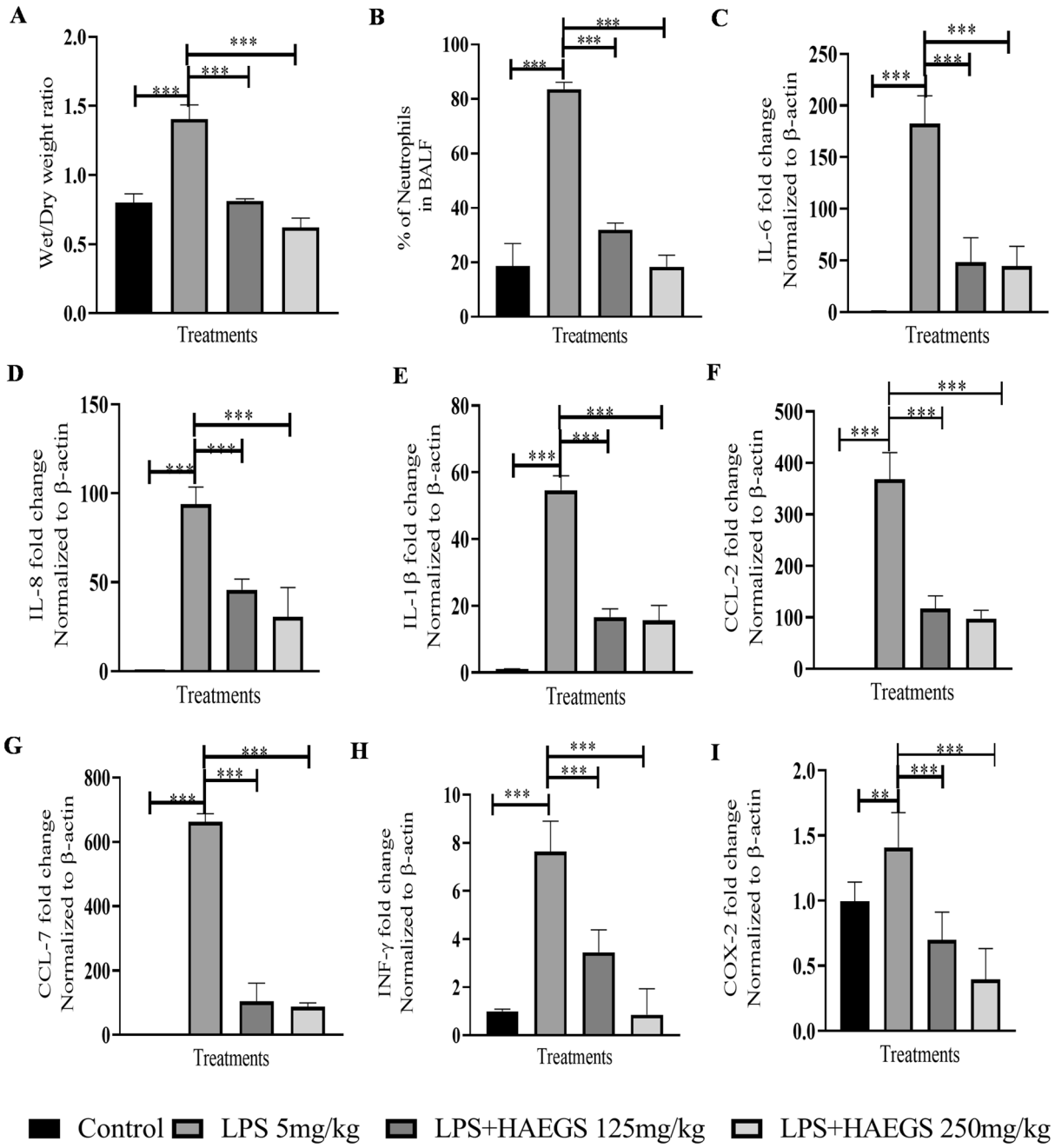

Fig. 4 Pre-treatment with HAEGS reduced the LPS-induced physiological changes and inflammatory responses in rat lungs. ARDS model was developed in male SD rats by intratracheal instillation of LPS (5 mg/kg). Post–pre-treatment, rats were challenged with LPS 5 mg/kg and then kept for 24 h monitoring. Thereafter, rats were anaesthetized and BALF fluid was collected from four rats for cell counting and lung tissue from four other animals for estimating the dry/wet ratio and qRT-PCR analysis for the specified primers. **A**, **B** Shows the effect of HAEGS against lipopolysaccharide (LPS)-induced elevation of lung wet-to-dry ratio (**A**) and neutrophil infiltration in bronchiolar lavage fluid (**B**). **C–I** Represents the mRNA expression of various inflammatory markers in rat lung tissues

HAEGS impeded LPS-induced oxidative stress in rat lung tissue samples

Oxidative stress is the leading cause of various metabolic and non-metabolic diseases, including several types of cancers, and acute lung, kidney and liver inflammations (Arslan et al. 2013; De Lima et al. 2013). To check whether HAEGS protects against LPS-induced oxidative stress, a nitric oxide estimation assay was performed using lung tissue samples. Nitric oxide assay results revealed that nitric

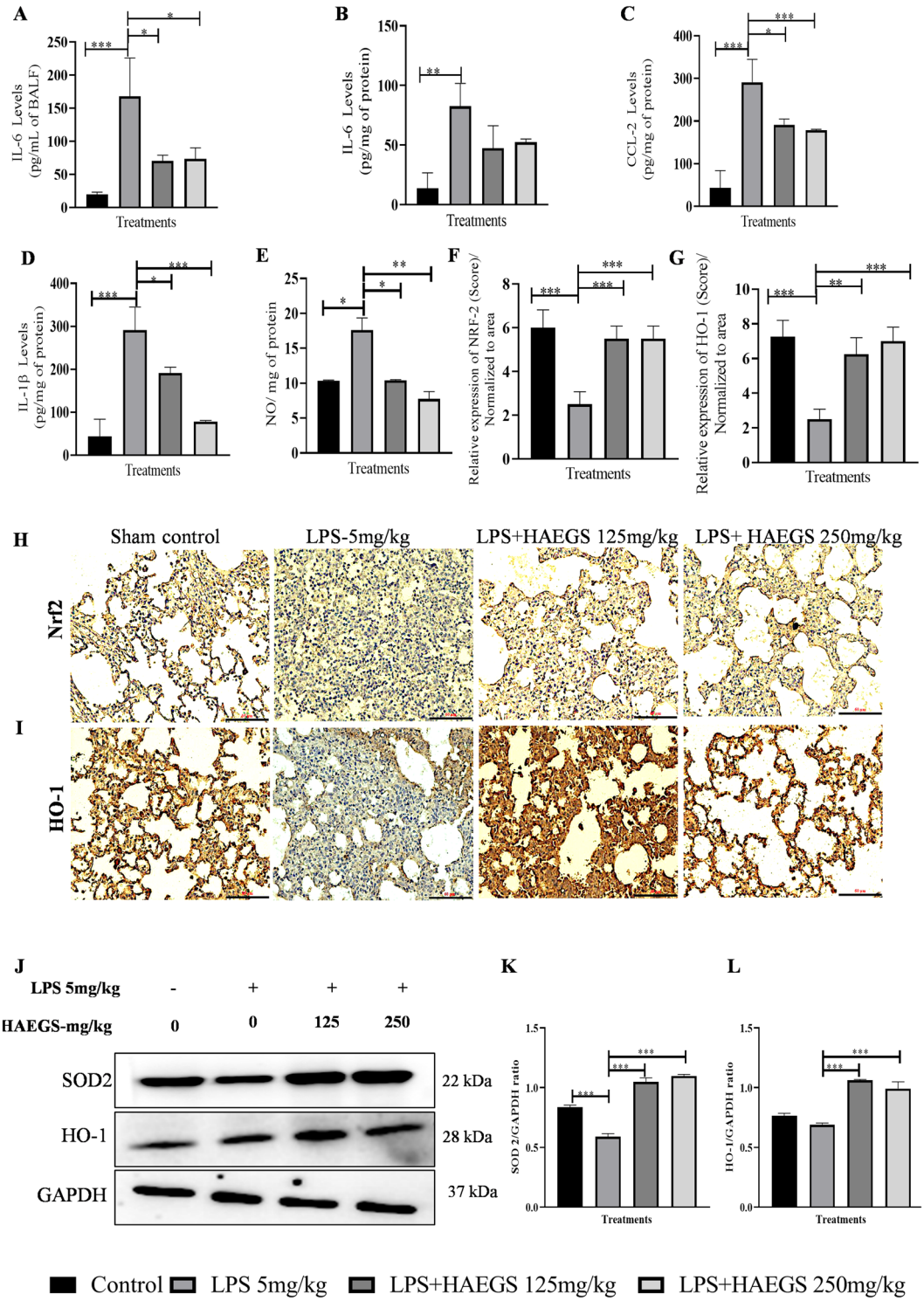

Fig. 5 HAEGS attenuated the inflammatory cytokine levels and oxidative stress mediators in LPS-stimulated lung tissue homogenates by modulating the Nrf2 pathway. After 24 h of treatment, BALF samples were collected and lungs were isolated. Further, BALF (**A**) and tissue samples (**B**–**D**) were subjected to ELISA for the specified protein estimations. A part of the tissues was homogenized and subjected to nitric oxide, for immunoblot and immunohistochemistry analysis for the specified antibodies. **E** Nitric oxide estimation. **F**, **G** Representative graphs of relative expression (immunohistochemistry score) on NRF-2 and HO-1 normalized to area. **H**, **I** Representative immunohistochemistry images of NRF-2 and HO-1. **J** Representative images of western blot analysis. **K** and **L** Graph represents densitometric quantification of the specified proteins. $*p<0.05$; $**p<0.01$; $***p<0.001$ vs. the LPS control group. Data represented as mean ± SEM, $n=8$. One-way ANOVA was performed for statistical analysis

oxide levels were significantly elevated in LPS control and the same was reduced in HAEGS pre-treated samples in a dose-dependent manner (Fig. 5E). Further to elucidate the underlying mechanism of HAEGS against oxidative stress, immunohistochemical analysis and Western blot analysis were performed for Nrf2 and its mediators. IHC results revealed that Nrf2 and HO-1 levels were remarkably reduced in LPS control tissues, and pre-treatment with HAEGS rescued the Nrf2 and HO-1 levels in a dose-dependent manner (Fig. 5F–I). Further, Western blot results confirmed that HO-1 and SOD levels were significantly reduced in LPS control and pre-treatment with HAEGS elevated the HO-1 and SOD levels in a dose-dependent manner (Fig. 5J–L).

HAEGS ameliorated the LPS-induced inflammatory markers expression by modulating the NF-κB/MAPK pathway

Further, to investigate the effect of HAEGS on inflammatory markers and identify the possible molecular mechanisms of the anti-inflammatory effect of HAEGS in-vivo models, lung tissue samples were subjected to western blot analysis. Western blot analysis revealed that TNF-α and MPO levels were significantly elevated upon LPS induction compared to sham control, wherein treatment with HAEGS significantly reduced the LPS-induced increase of TNF-α and MPO levels in a dose-dependent manner (Fig. 6A–C). Next, we investigated the effect of HAEGS on MUC5AC, as it is the downstream target of the MAPKinase pathway and is well known to play a vital role in the pathogenesis of airway diseases among other mucins. Western blot analysis revealed that MUC5AC levels were significantly elevated in LPS control samples, whereas in the HAEGS-treated samples, MUC5AC expression levels were significantly reduced (Fig. 6A and D). Mechanistic investigation revealed that phosphorylated p65, p38, JNK, and ERK, levels were significantly increased in the LPS control samples compared to sham control and treatment with HAEGS significantly reduced the phospho-p65, phospho-p38, phospho-ERK and phosphor-JNK compared to the LPS control tissues (Fig. 6A and E–H). Overall, these results indicated that pre-treatment with HAEGS reversed the MPO, TNF-α and MUC5AC expression through modulating the NF-κB and MAPK signalling, impeding inflammatory response.

HAEGS treatment protected the LPS-induced lung injury and ameliorates the pathological changes

LPS treatment was reported to cause severe damage to the lungs when administered intratracheally into the lungs, which involves induction of interstitial inflammation, oedema and lymphoid infiltration in just 4 h after its administration (Seemann et al. 2017). To investigate whether HAEGS ameliorates LPS induced pathological changes or not, lung tissues were subjected to H&E analysis and PAS staining. H&E analysis revealed that LPS induced elevated interstitial inflammation, infiltration of neutrophils in the alveolar interstitial space, alveolar inflammation, wall thickening, severe oedema and periarteriolar inflammation with infiltration of various inflammatory cells, in LPS control animal lung tissues. Treatment with HAEGS significantly reduced the LPS-induced pathological abnormalities in lung tissues (Fig. 7A and E). To further confirm that HAEGS could ameliorate the LPS-induced lung injury, PAS staining was performed using lung tissue sections. PAS analysis revealed that the per cent of PAS-positive goblet cells were remarkably upregulated by LPS instillation, whereas reversed in HAEGS pre-treatment in a dose-dependent manner (Fig. 7B and F). The above data demonstrated that HAEGS exhibited a protective role against the LPS-induced ALI in rat models.

HAEGS attenuated the expression of neutrophil elastase and myeloperoxidase in lung tissues

Elevated extracellular release of neutrophil granular enzymes plays a crucial role in cytokine storm-mediated lung damage. Neutrophil elastase (NE) degrades the pulmonary ECM proteins and cleaves the respiratory cell–cell adhesion (Yang et al. 2021). Myeloperoxidase (MPO) activity is potentiated by NE and plays a major role in acute inflammation in the lungs. It was reported that MPO, an abundant enzyme released from neutrophil granules, modulates the course of acute pulmonary inflammatory responses induced by LPS administration. To determine the effect of HAEGS against LPS-induced ARDS, lung tissue sections were subjected to immunohistochemistry (IHC) against neutrophil elastase and MPO. IHC results revealed that LPS stimulation increased the NE and MPO levels significantly in LPS control and treatment with HAEGS significantly ameliorated the LPS elevated levels of NE (Fig. 7C and G) and MPO (Fig. 7D and H) in a dose-dependent manner.

Fraction 6 of HAEGS attenuated the LPS-induced pro-inflammatory markers

Since HAEGS is a whole GS leave extract, it contains several types of compounds. To determine the active ingredients which are responsible for therapeutic effect, we used the silica column chromatography method to separate various compounds based on their polarity starting with non-polar molecules. About 30 fractions were pooled into 6 major fractions based on the TLC plate readings (Fig. S8B). All six fractions were tested for their anti-inflammatory properties along with known main active ingredients of *Gymnema Sylvestre* such as gymnemagenin and deacyl gymnemic

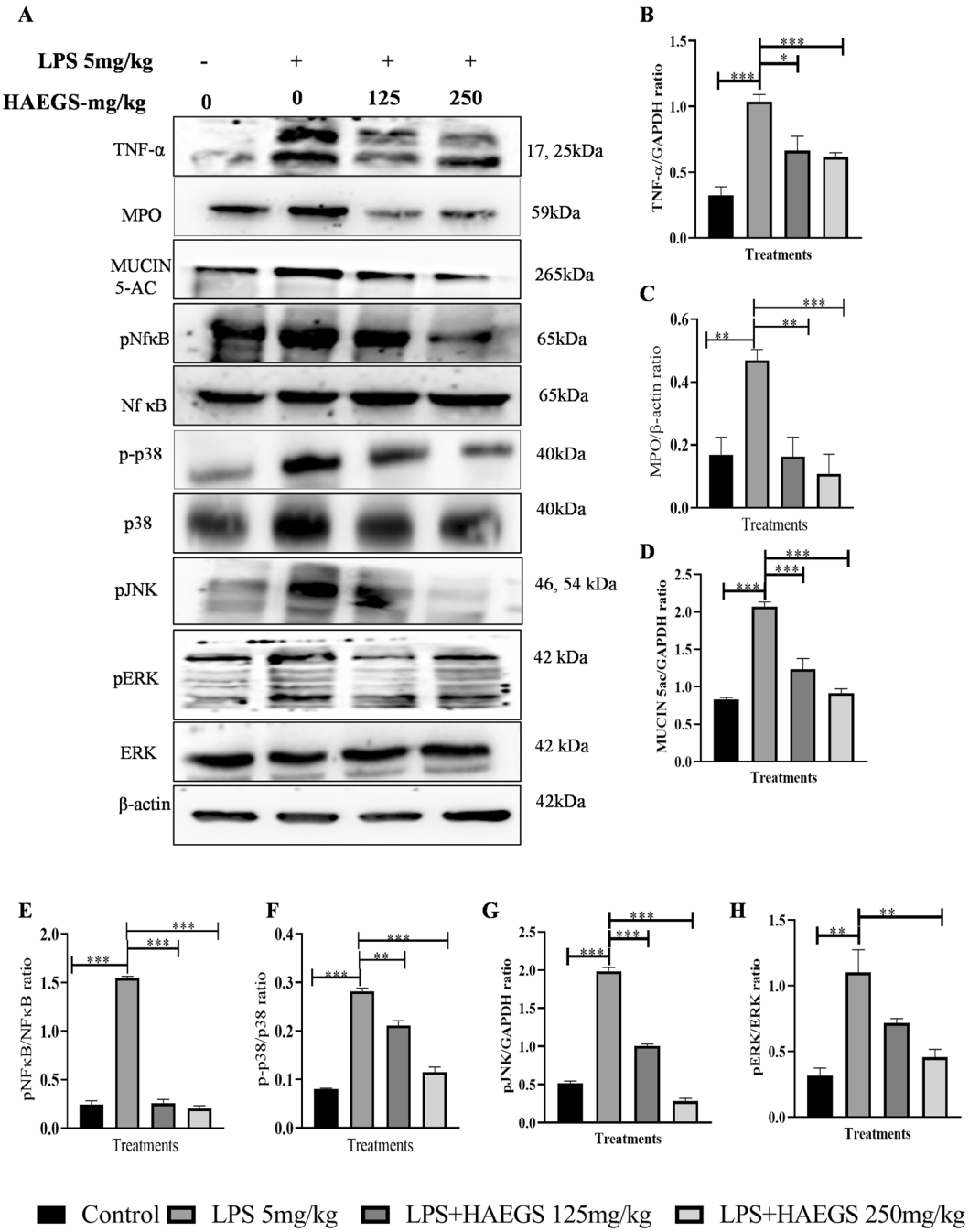

Fig. 6 HAEGS abrogated the expression of inflammatory markers by modulating the NF-κB and MAPK pathway. After the treatment period, lung tissues were collected, and part of the tissues were homogenized and subjected to immunoblot analysis for the specified proteins. **A** Representative images of Western blot. **B**–**H** Graph represents densitometric quantification of the specified proteins; nitric oxide estimation (M). $*p<0.05$; $**p<0.01$; $***p<0.001$ vs. the LPS control group. Data represented as mean ± SEM, $n=8$. One-way ANOVA was performed for statistical analysis

acid. The isolated fractions were subjected to a cell viability assay prior to performing the anti-inflammatory activity, and the results revealed that fraction 6 treated cells were (above 95%) viable in all tested concentrations, whereas other fractions (fractions 1–5) showed above 95% viability at 25 µg/mL only and showed less viability in above 25 µg/mL concentrations (Table. S9). Further, these fractions (25 µg/mL) were subjected to RT-qPCR analysis to evaluate their anti-inflammatory activity, and the results showed that only fraction 6 (F6) significantly decreased the levels of IL-1β

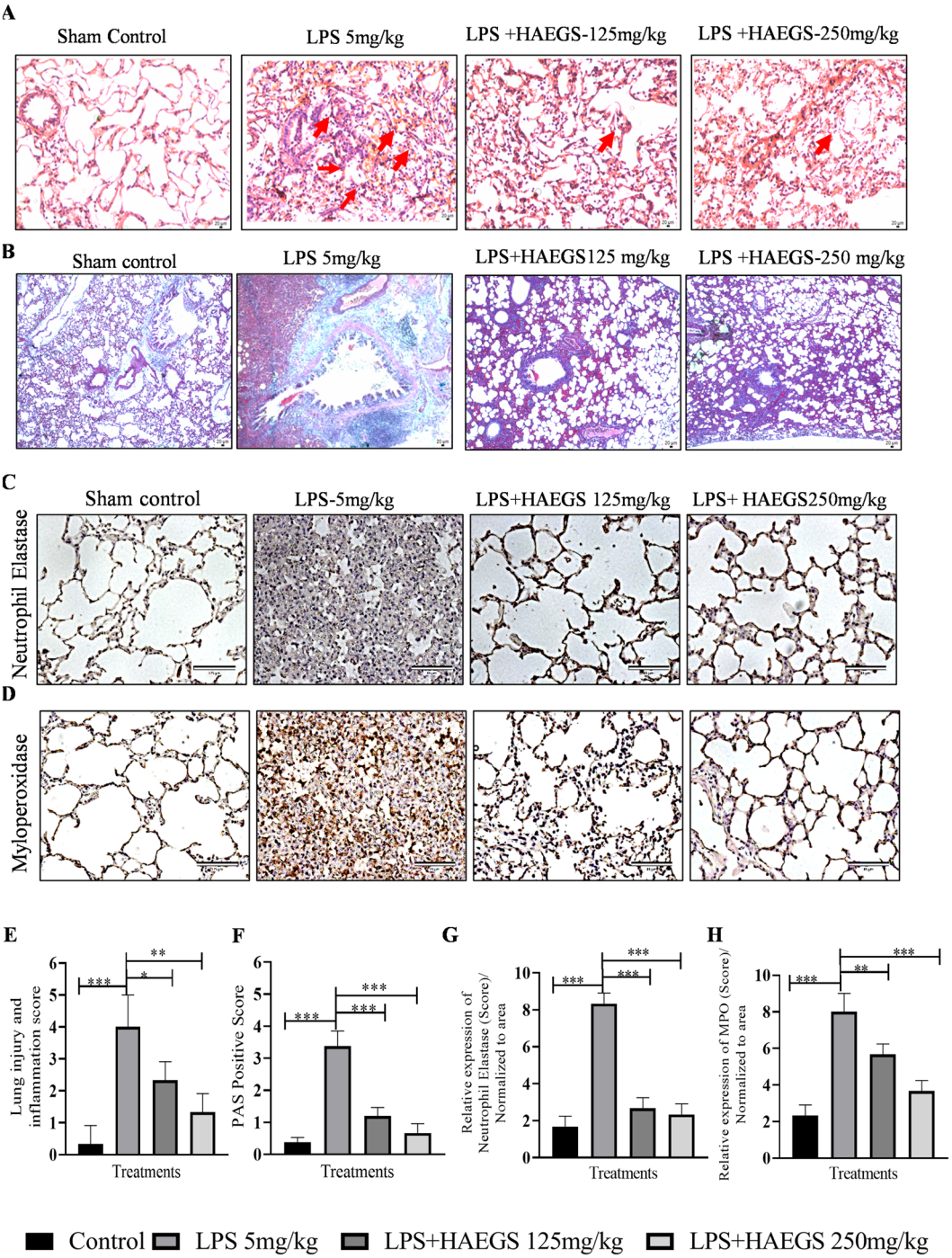

Fig. 7 HAEGS treatment ameliorated the infiltration of inflammatory cells, pathological changes and neutrophil-mediated events in LPS-stimulated lung tissues. After the treatment period, the lungs were subjected to histopathology. **A** Representative images (10×) of H&E staining, the red arrow points at typical areas of inflammation, manifesting oedema and infiltration of inflammatory cells. Graphs represent the score of (**E**) lung injury and inflammation score. PAS staining was used to observe goblet cells in LPS-induced rats with acute lung injury. **B** Representative images (10x) of PAS staining. Goblet cells were identified using PAS in LPS-induced rat lungs. **F** The quantification of the PAS-positive score. **C**, **D**, **G** and **H** Representative IHC images of neutrophil elastase (**C**) and myeloperoxidase (**D**), quantification of neutrophil elastase expression (**G**) and quantification of MPO expression (**H**) in the lung sections. Images were taken under 20×magnification. $n=8$ $*p<0.05$; $**p<0.01$; $***p<0.001$ vs. the LPS control group. Data represented as mean ± SEM. One-way ANOVA was performed for statistical analysis

and IL-6 in LPS-stimulated BEAS-2B cells when compared to the control (Fig. 8A and B). Interestingly, fraction 6 treatment demonstrated superior suppression of IL-6 and IL-1β than HAEGS. To understand the molecular composition of fraction 6, we carried out different mass spectrometry analyses. A total of 14 metabolites were identified and all metabolites corresponded to gymnemic acid: deacyl gymnemic acid II, gymnemic acid I, IV–X, XIII, XIV and XVII (Fig. 8C, Fig. S9 and Table 1). Overall, our findings demonstrated that fraction 6 of HAEGS contains components that are active in decreasing ARDS via the NF-κB/MAPK pathway regulation of pro-inflammatory marker expression.

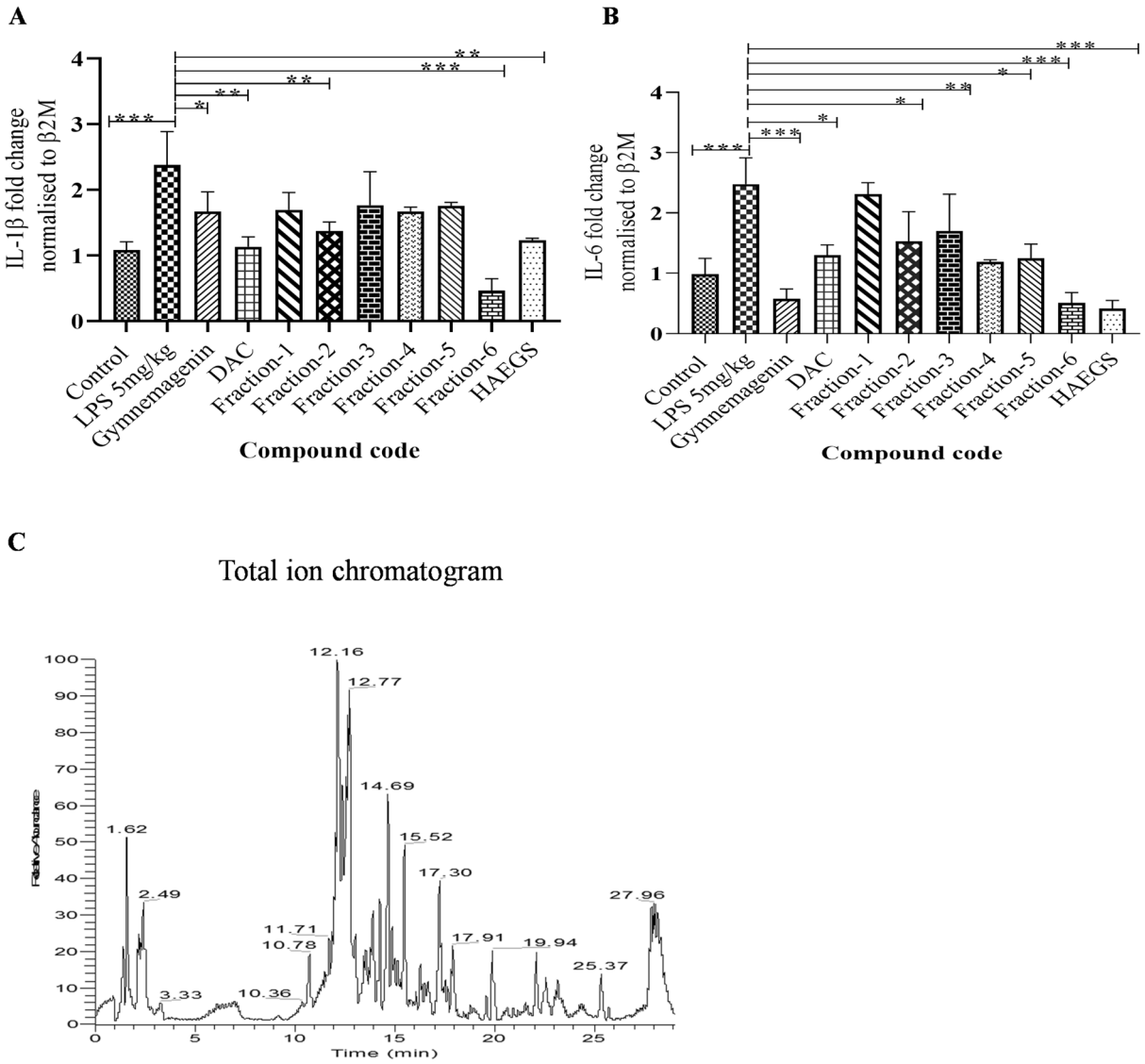

Fig. 8 Fraction 6 metabolites significantly inhibited the IL-6 and IL-1β expression levels in BEAS-2B cells. **A** and **B** BEAS-2B cells were cultured in serum-free media for 6 h, then cells were pre-treated with various fractions of HAEGS (25 µg/mL) or deacyl gymnemic acid or gymnemagenin or (100 µg/mL) or whole HAECS (125 µg/mL) for a period of 2 h, then cells were stimulated with LPS (5 µg/mL) for a period of 12 h. Thereafter, cells were subjected to qRT-PCR analysis using specified primer sets. Graphs in panels represent fold change in gene expression normalized to β2M. C) Molecular composition of fraction 6 was carried out by loading the fraction 6 of HAEGS chromatographic separations on a Surveyor UHPLC system using a Syncronis C18 column (2.1 × 100 mm; Thermo Scientific, Germany) column with a gradient mobile phase of 0.1% formic acid in water and acetonitrile with a flow rate of 0.15 mL/min. $*p < 0.05$, $**p < 0.01$, $***p < 0.001$. *NS* non-significant. One-way ANOVA was performed for statistical analysis. Data represented as mean ± SEM, $n = 3$

Table 1 Secondary metabolites identified from HAEGS using LC–HRMS under negative ionization modes in fraction 6

S. no.	Compound name	Chemical formula $[M-H]^-$	Experimental *m/z*	Theoretical *m/z*	Mass error (Δ ppm)	RT (min)
1	Gymnemic acid I	$C_{43}H_{65}O_{14}$	805.4339	805.4374	−3.70	22.48
2	Deacyl Gymnemic acid II	$C_{36}H_{57}O_{12}$	681.4183	681.3821	−3.72	19.76
3	Gymnemic acid IV	$C_{41}H_{63}O_{13}$	763.4232	763.4269	−4.05	21.05
4	Gymnemic acid V	$C_{46}H_{71}O_{14}$	845.4641	845.4844	−4.87	23.57
5	Gymnemic acid VI	$C_{47}H_{73}O_{18}$	925.4755	925.4797	−3.39	22.50
6	Gymnemic acid IX	$C_{47}H_{71}O_{18}$	923.4598	923.4640	−4.19	21.35
7	Gymnemic acid X	$C_{38}H_{59}O_{13}$	723.3926	723.3956	−3.31	18.75
8	Gymnemic acid XIII	$C_{41}H_{65}O_{13}$	765.4391	765.4425	−3.79	21.38
9	Gymnemic acid XIV	$C_{41}H_{63}O_{13}$	763.4232	763.4269	−4.08	20.94
10	Gymnemic acid XVII	$C_{43}H_{61}O_{13}$	785.4061	785.4112	−3.24	21.29
11	Gymnemagenin	$C_{30}H_{49}O_6$	505.3539	505.3529	3.12	17.56
12	Rutin	$C_{27}H_{29}O_{16}$	609.1432	609.1456	−2.96	15.50
13	Conduritol	$C_6H_9O_5$	161.04446	161.0450	1.05	14.59
14	Gymnemoside-C	$C_{45}H_{63}O_{14}$	827.4174	827.4218	−4.67	22.71

Discussion

Various studies have indicated that inflammatory cytokines exert significant effects on the induction and maintenance of inflammatory diseases which require immediate medical attention. Recent pandemic SARC-CoV-2 infection is extremely variable, ranging from no or mild symptoms to severe acute respiratory distress syndrome (Menzella et al. 2020). In several COVID-19 patients, ARDS-induced cytokine storm leads to partial to complete lung damage, resulting in mortality (Hojyo et al. 2020). Several treatment modalities are practised in clinics to mitigate the cytokine storm including the administration of steroids and cytokine-specific monoclonal antibodies. Though corticosteroids play a prominent role in mitigating the cytokine storm in the early stages of infection, they could cause several side effects due to immune suppression that could lead to even death (Tang et al. 2020a). Tocilizumab treatment showed some promising results in COVID-19 patients with severe respiratory impairment receiving non-invasive mechanical ventilation. However, few patients developed cavitating lung lesions during the follow-up period, which implies that though tocilizumab treatment is beneficial, it could have serious side effects in some patients (Menzella et al. 2020). It was reported that patients with elevated plasma levels of IL-6, IL-8, TNF-α and IL-1β on day 1 of ARDS had a persistent increase of these inflammatory cytokines over time, leading to mortality (Meduri et al. 1995).

In this study, pre-treatment with HAEGS significantly reduced the LPS-induced cytokines (*IL-6*, *IL-1β*, *TNF-α*), chemokines (*CCL-7*, *CXCL-8*), inflammatory marker (*COX-2*) and macrophage marker (*F4/80*) expressions in a dose-dependent manner. In numerous lung injury models, the biomarkers *VCAM-1* and *ICAM-1* indicate endothelial damage (Spadaro et al. 2021). We show that HAEGS pre-treatment significantly mitigated the *ICAM-1* and *VCAM*-1 expression in LPS-stimulated lung epithelial cells. It was reported that stimulation of macrophages or epithelial cells with LPS, generates ROS, which contributes to severe inflammation and leads to the elevation of inflammatory markers that may cause damage to the target organs (Liu et al. 2018). Pre-treatment with HAEGS reduced the ROS levels which were gauged by DCFDA analysis and nitric oxide assay. It has been shown that the activation of NF-κB by LPS treatment is followed by a cascade of events, leading to the activation of several signalling pathways, including PI3K/Akt and MAPKs that are crucial for regulating inflammation and releasing the inflammatory factors (Jung et al. 2017). Accumulated data suggest that stimulation of macrophages with LPS leads to activation of the MAPK (ERK, JNK, and p38) pathway (Van Der Bruggen et al. 1999). LPS stimulation elevates the phosphorylation of extracellular signal-regulated kinase (ERK) 1/2 and enhances the expression of TNF-α in RAW-264.7 murine macrophages (Shi et al. 2002). JNK and p38 (MAPK pathway) are mainly activated by bacterial LPS and subsequently by inflammatory cytokines such as TNF-α and IL-1β (Ono and Han 2000). To determine whether NF-κB and MAPK signalling pathways are involved in the HAEGS-induced inhibition of the inflammatory response, the effects of HAEGS on the activation of the p65, p38, JNK and ERK were investigated. Our results revealed that the LPS-induced phosphorylation of p38, ERK, JNK and p65 were markedly suppressed by pre-treatment with HAEGS. This study's multiple lines of evidence support that HAEGS pre-treatment significantly

attenuated the LPS-induced inflammatory cascade in macrophages and lung epithelial cells.

Several investigations have shown that elevated lung wet-to-dry weight ratio, exuberant neutrophil infiltration and leukocyte accumulation in BALF samples after 24 h of LPS administration are essential pathological characteristics of ARDS (Li et al. 2016a; Tseng et al. 2012). Neutrophils play a critical role in the initiation, propagation and resolution of this complex inflammatory environment by infiltrating into the lung and executing a distinct pro-inflammatory function. These include the release of cytokines and reactive oxygen species as well as the production of neutrophil extracellular traps. It has been shown that the number of neutrophils in the BALF of patients with ARDS correlates closely with the severity of the disease (Steinberg et al. 1994), while depletion of polymorphonuclear neutrophils (PMN) in animal models ameliorates lung injury with reduced capillary–alveolar permeability and epithelial cell damage (Abraham et al. 2000). In the current study, intratracheal instillation of LPS in rats led to a marked increase in lung dry wet-to-dry ratio and infiltration of neutrophils in BALF samples. On the other hand, pre-treatment with HAEGS significantly mitigated the same, thus ameliorating lung oedema and neutrophil infiltration. Pro-inflammatory chemokines such as *IL-8, CCL2*, and *CCL7* are produced by macrophages or epithelial cells primarily to recruit neutrophils and leukocytes to the affected organs (Turner et al. 2014). Our investigation revealed an increase in cytokine and chemokine levels in LPS control animals and pre-treatment with HAEGS significantly mitigated these events in a dose-dependent manner.

The Nrf2 pathway is crucial for maintaining the cellular redox homeostasis (Ci et al. 2017) and maintaining oxidative stress. Recent studies have shown that Nrf2 activation is crucial for ARDS patients to manage oxidative stress and inflammation (Liu et al. 2019). It has been reported that Nrf2 activation protected the LPS (intratracheal administration)-induced acute respiratory distress syndrome in mice by modulating the macrophage polarization (Wei et al. 2018). It was also reported that heme oxygenase-1 (HO-1) is a stress-inducible protein that plays a crucial role in protective mechanisms against oxidative stress (Yu et al. 2016). Similar to reported studies, our study results revealed that LPS stimulation significantly increased the nitric oxide levels and reduced the Nrf2, HO-1 and SOD levels. Interestingly pre-treatment with HAEG mitigated the nitric oxide levels and rescued the Nrf2, HO-1 and SOD levels, indicating that HAEGS suppressed the LPS-induced oxidative stress through suppressing the Nrf2 pathway.

Next, we examined the underlying mechanism(s) by which HAEGS mitigates LPS-induced neutrophil infiltration, cytokine expression, elastase expression, myeloperoxidase levels and lung injury in lung tissues. Our investigation of lung tissue samples revealed that LPS elevated the MPO, TNF-α levels and phosphorylation of p65 and p38, and pre-treatment with HAEGS significantly reduced the same in a dose-dependent manner. It was reported that inhibition or knockdown of p38 or ERK (MAPkinase pathway) attenuates the cytokine (IL-1β and TNF-α)-induced MUC5AC expression in epithelial cells (Song et al. 2003). Similarly, our study also showed that HAEGS pre-treatment reduced the expression of MUC5AC by modulating the pro-inflammatory cytokines and MAPK pathway. The lung histopathological analysis was similar to our previous study (Tirunavalli et al. 2021a), which demonstrated that alveolar septal thickening, interstitial oedema and vascular congestion were elevated in the LPS control, all of which were relieved by HAEGS pre-treatment. Further PAS staining results exhibited that HAEGS rescued the LPS-induced upregulation of PAS-positive cells in a dose-dependent manner. Elevated levels of MPO in pulmonary parenchyma, reflecting the activation of neutrophils, were largely overexpressed in acute lung injury conditions (Dong and Yuan 2018). Substantial pieces of evidence have confirmed that increased NE levels are an indispensable contributor to the progression of acute lung injury and its deleterious actions are noticeable in lung tissues (Tsai et al. 2015). Administration of HAEGS significantly reduced both MPO and Ne levels in a dose-dependent manner, suggesting that, HAEGS treatment may ameliorate the neutrophil-mediated damage in lung tissues.

According to characterization studies, the major components in the HAEGS were identified as gymnemic acid, gymnemasaponins, gymnemoside, gymnemasin, quercetin, palmitic acid, stearic acid, linolenic acid, octadecenoic acid, stearin, squalene and γ-tocopherol. Most of these molecules are known for their anti-inflammatory and antioxidant property which directly or indirectly are implicated in the suppression of inflammatory cytokines (Alkhatib et al. 2019). Different derivatives of gymnemasaponins suppress the glucose uptake indirectly demonstrating the antioxidant property (Yoshikawa et al. 1991, 2000). Anti-inflammatory and immune-modulating activity has been identified for quercetin in various animal models by reducing visceral adipose tissue, TNF-α and nitric oxide production, in addition to downregulating nitric oxide synthase (NOS) production in obese Zucker rats (Rivera et al. 2008). γ-Tocopherol is known to reduce the oxidative stress in the brain induced by the reactive nitrogen species (RNS) (Pahrudin Arrozi et al. 2020). Further, fractionation studies have revealed that only fraction 6 (F6) showed anti-inflammatory activity among other fractions. Further analysis of the molecular components suggested that F6 contained different derivatives of only gymnemic acid.

Overall, in the current study, we demonstrate that hydroalcoholic extract of *Gymnema Sylvestre* strongly attenuates LPS-induced cytokines expression, ROS levels in in vitro and in vivo models and PMN infiltration, thus rescuing the

rats against LPS-induced ALI. We have further discovered that HAEGS significantly reduces lung injury, MPO and neutrophil elastase levels by modulating the NF-κB/MAPK pathway. Major active ingredients that are responsible for the observed function are gymnemic acid and its derivatives.

Conclusion

Cytokine storm/ARDS is a critical phase of viral or bacterial infection of the lungs. *Gymnema Sylvestre* hydroalcoholic extract, which functions as an antioxidant and anti-inflammatory formulation, defends against the cytokine storm in the LPS-induced ARDS model by suppressing the Nrf2 mediators and modulating the NF-κB/MAPK pathway. Either entire HAEGS or fraction 6 (F6) with a gymnemic acid enrichment could be used as a phytochemical medication to treat ARDS and other inflammatory lung injuries.

Supplementary Information The online version contains supplementary material available at https://doi.org/10.1007/s10787-022-01133-5.

Acknowledgements The authors thank the Director, CSIR-IICT, Hyderabad, India, for providing the facilities and funding necessary for conducting this work. AJ thanks the Council of Scientific and Industrial Research (CSIR), New Delhi, India, for the award of Research Associate (RA) and SKT thanks the ICMR, New Delhi, India, for the award of senior research fellow (SRF). CSIR-IICT manuscript communication number: IICT/Pubs./2021/386.

Author contributions Conceptualization: AA and SBA. Methodology: AJ, TSK, SBA, AA. Preparation and analysis of extract: BMA, BK, Analysis of extract: SSP, JRT. Validation: AA, SBA. In vitro cell culture: AJ and SKT. RT-qPCR, Western blot analysis, ex vivo and in vivo experiments: AJ, TSK. Immunohistochemistry analysis: AJ and TSK. Pathological studies: EJ. Manuscript writing—review and editing: SBA, AA. Funding acquisition: AA and SBA.

Funding Used internal funds of the CSIR-Indian Institute of Chemical Technology, Hyderabad. This research did not receive any specific grant from funding agencies in the public, commercial, or not-for-profit sectors.

Data availability All data generated or analysed for this study are included in this manuscript file (and its supplementary information files).

Declarations

Conflict of interest The authors declare no competing or financial interests.

References

Abraham E, Carmody A, Shenkar R, Arcaroli J (2000) Neutrophils as early immunologic effectors in hemorrhage- or endotoxemia-induced acute lung injury. Am J Physiol Lung Cell Mol Physiol 279:L1137–L1145. https://doi.org/10.1152/ajplung.2000.279.6.L1137

Alavinezhad A, Hedayati M, Boskabady MH (2017) The effect of Zataria multiflora and carvacrol on wheezing, FEV1 and plasma levels of nitrite in asthmatic patients. Avicenna J Phytomed 7:531–541

Aleisa AM, Al-Rejaie SS, Abuohashish HM, Ola MS, Parmar MY, Ahmed MM (2014) Pretreatment of *Gymnema sylvestre* revealed the protection against acetic acid-induced ulcerative colitis in rats. BMC Complement Altern Med 14:49. https://doi.org/10.1186/1472-6882-14-49

Alkhatib A, Tuomilehto JJEOED (2019) Lifestyle diabetes prevention. Elsiver

Andugulapati SB, Gourishetti K, Tirunavalli SK, Shaikh TB, Sistla R (2020) Biochanin-A ameliorates pulmonary fibrosis by suppressing the TGF-β mediated EMT, myofibroblasts differentiation and collagen deposition in in vitro and in vivo systems. Phytomedicine 78:153298. https://doi.org/10.1016/j.phymed.2020.153298

Arslan F, Lai RC, Smeets MB, Akeroyd L, Choo A, Aguor EN, Timmers L, Van Rijen HV, Doevendans PA, Pasterkamp G, Lim SK, De Kleijn DP (2013) Mesenchymal stem cell-derived exosomes increase ATP levels, decrease oxidative stress and activate PI3K/Akt pathway to enhance myocardial viability and prevent adverse remodeling after myocardial ischemia/reperfusion injury. Stem Cell Res 10:301–312. https://doi.org/10.1016/j.scr.2013.01.002

Aslan A, Aslan C, Zolbanin NM, Jafari R (2021) Acute respiratory distress syndrome in COVID-19: possible mechanisms and therapeutic management. Pneumonia 13:14. https://doi.org/10.1186/s41479-021-00092-9

Bachofen M, Weibel ER (1977) Alterations of the gas exchange apparatus in adult respiratory insufficiency associated with septicemia. Am Rev Respir Dis 116:589–615. https://doi.org/10.1164/arrd.1977.116.4.589

Baird L, Yamamoto M (2020) The molecular mechanisms regulating the KEAP1-NRF2 pathway. Mol Cell Biol. https://doi.org/10.1128/mcb.00099-20

Barnes PJ, Adcock I (1993) Anti-inflammatory actions of steroids: molecular mechanisms. Trends Pharmacol Sci 14:436–441. https://doi.org/10.1016/0165-6147(93)90184-l

Baskaran K, Kizar Ahamath B, Radha Shanmugasundaram K, Shanmugasundaram ER (1990) Antidiabetic effect of a leaf extract from *Gymnema sylvestre* in non-insulin-dependent diabetes mellitus patients. J Ethnopharmacol 30:295–300. https://doi.org/10.1016/0378-8741(90)90108-6

Chousterman BG, Swirski FK, Weber GF (2017) Cytokine storm and sepsis disease pathogenesis. Semin Immunopathol 39:517–528. https://doi.org/10.1007/s00281-017-0639-8

Ci X, Zhou J, Lv H, Yu Q, Peng L, Hua S (2017) Betulin exhibits anti-inflammatory activity in LPS-stimulated macrophages and endotoxin-shocked mice through an AMPK/AKT/Nrf2-dependent mechanism. Cell Death Dis 8:e2798–e2798. https://doi.org/10.1038/cddis.2017.39

Dadinaboyina SB, Yerra NV, Adimoolam BM, Parsa S, Bathini NB, Thota JR (2021) Identification and characterization of degradation products of Remdesivir using liquid chromatography/mass spectrometry. New J Chem 45:7217–7224. https://doi.org/10.1039/D1NJ00160D

De Lima FM, Albertini R, Dantas Y, Maia-Filho AL, Santana Cde L, Castro-Faria-Neto HC, França C, Villaverde AB, Aimbire F (2013) Low-level laser therapy restores the oxidative stress balance in acute lung injury induced by gut ischemia and reperfusion. Photochem Photobiol 89:179–188. https://doi.org/10.1111/j.1751-1097.2012.01214.x

Determann RM, Millo JL, Waddy S, Lutter R, Garrard CS, Schultz MJ (2009) Plasma CC16 levels are associated with development of ALI/ARDS in patients with ventilator-associated pneumonia:

a retrospective observational study. BMC Pulm Med 9:49–49. https://doi.org/10.1186/1471-2466-9-49

Dong Z, Yuan Y (2018) Accelerated inflammation and oxidative stress induced by LPS in acute lung injury: Inhibition by ST1926. Int J Mol Med. https://doi.org/10.3892/ijmm.2018.3574

Hojyo S, Uchida M, Tanaka K, Hasebe R, Tanaka Y, Murakami M, Hirano T (2020) How COVID-19 induces cytokine storm with high mortality. Inflamm Regener 40:37–37. https://doi.org/10.1186/s41232-020-00146-3

Jung J-S, Choi M-J, Lee YY, Moon B-I, Park J-S, Kim H-S (2017) Suppression of lipopolysaccharide-induced neuroinflammation by Morin via MAPK, PI3K/Akt, and PKA/HO-1 signaling pathway modulation. J Agric Food Chem 65:373–382. https://doi.org/10.1021/acs.jafc.6b05147

Kanetkar P, Singhal R, Kamat M (2007a) *Gymnema sylvestre*: a memoir. J Clin Biochem Nutr 41:77–81. https://doi.org/10.3164/jcbn.2007010

Kanetkar P, Singhal R, Kamat M (2007b) *Gymnema sylvestre*: a memoir. J Clin Biochem Nutr 41:77–81. https://doi.org/10.3164/jcbn.2007010

Kany S, Vollrath JT, Relja B (2019) Cytokines in inflammatory disease. Int J Mol Sci 20:6008. https://doi.org/10.3390/ijms20236008

Khiali S, Khani E, Entezari-Maleki T (2020) A comprehensive review of tocilizumab in COVID-19 acute respiratory distress syndrome. J Clin Pharmacol 60:1131–1146. https://doi.org/10.1002/jcph.1693

Lawrence T (2009) The nuclear factor NF-κB pathway in inflammation. Cold Spring Harb Perspect Biol 1:a001651. https://doi.org/10.1101/cshperspect.a001651

Leach MJ (2007) *Gymnema sylvestre* for diabetes mellitus: a systematic review. J Altern Complement Med 13:977–983. https://doi.org/10.1089/acm.2006.6387

Li L, Maitra U, Singh N, Gan L (2010) Molecular mechanism underlying LPS-induced generation of reactive oxygen species in macrophages. FASEB J 24:422.3. https://doi.org/10.1096/fasebj.24.1_supplement.422.3

Li Y, Huang J, Foley NM, Xu Y, Li YP, Pan J, Redmond HP, Wang JH, Wang J (2016a) B7H3 ameliorates LPS-induced acute lung injury via attenuation of neutrophil migration and infiltration. Sci Rep 6:31284. https://doi.org/10.1038/srep31284

Li Y, Yao J, Han C, Yang J, Chaudhry MT, Wang S, Liu H, Yin Y (2016b) Quercetin, inflammation and immunity. Nutrients 8:167

Li Y, Xiao Y, Gao W, Pan J, Zhao Q, Zhang Z (2019) Gymnemic acid alleviates inflammation and insulin resistance via PPARδ- and NFκB-mediated pathways in db/db mice. Food Funct 10:5853–5862. https://doi.org/10.1039/C9FO01419E

Liu Z, Ren Z, Zhang J, Chuang C-C, Kandaswamy E, Zhou T, Zuo LJFIP (2018) Role of ROS and nutritional antioxidants in human diseases. Front Physiol 9:477

Liu Q, Gao Y, Ci X (2019) Role of Nrf2 and its activators in respiratory diseases. Oxid Med Cell Longev 2019:7090534. https://doi.org/10.1155/2019/7090534

Malik J, Manvi F, Alagawadi K, Noolvi MJIJOGP (2008) Evaluation of anti-inflammatory activity of *Gymnema sylvestre* leaves extract in rats. Int J Green Pharmacy 2:114

Manicone AM (2009) Role of the pulmonary epithelium and inflammatory signals in acute lung injury. Expert Rev Clin Immunol 5:63–75. https://doi.org/10.1586/177666X.5.1.63

Meduri GU, Headley S, Kohler G, Stentz F, Tolley E, Umberger R, Leeper K (1995) Persistent elevation of inflammatory cytokines predicts a poor outcome in ARDS. Plasma IL-1β and IL-6 levels are consistent and efficient predictors of outcome over time. Chest 107:1062–1073. https://doi.org/10.1378/chest.107.4.1062

Menzella F, Fontana M, Salvarani C, Massari M, Ruggiero P, Scelfo C, Barbieri C, Castagnetti C, Catellani C, Gibellini G, Falco F, Ghidoni G, Livrieri F, Montanari G, Casalini E, Piro R, Mancuso P, Ghidorsi L, Facciolongo N (2020) Efficacy of tocilizumab in patients with COVID-19 ARDS undergoing noninvasive ventilation. Crit Care 24:589. https://doi.org/10.1186/s13054-020-03306-6

Merad M, Martin JC (2020) Pathological inflammation in patients with COVID-19: a key role for monocytes and macrophages. Nat Rev Immunol 20:355–362. https://doi.org/10.1038/s41577-020-0331-4

Ogata-Suetsugu S, Yanagihara T, Hamada N, Ikeda-Harada C, Yokoyama T, Suzuki K, Kawaguchi T, Maeyama T, Kuwano K, Nakanishi Y (2017) Amphiregulin suppresses epithelial cell apoptosis in lipopolysaccharide-induced lung injury in mice. Biochem Biophys Res Commun 484:422–428. https://doi.org/10.1016/j.bbrc.2017.01.142

Ono K, Han J (2000) The p38 signal transduction pathway: activation and function. Cell Signal 12:1–13. https://doi.org/10.1016/s0898-6568(99)00071-6

Pahrudin Arrozi A, Shukri SNS, Wan Ngah WZ, Mohd Yusof YA, Ahmad Damanhuri MH, Jaafar F, Makpol S (2020) Comparative effects of α- and γ-tocopherol on mitochondrial functions in Alzheimer's disease in vitro model. Sci Rep 10:8962. https://doi.org/10.1038/s41598-020-65570-4

Proudfoot AG, Mcauley DF, Griffiths MJD, Hind M (2011) Human models of acute lung injury. Dis Model Mech 4:145–153. https://doi.org/10.1242/dmm.006213%JDiseaseModels&Mechanisms

Rivera L, Morón R, Sánchez M, Zarzuelo A, Galisteo M (2008) Quercetin ameliorates metabolic syndrome and improves the inflammatory status in obese Zucker rats. Obesity (silver Spring) 16:2081–2087. https://doi.org/10.1038/oby.2008.315

Sahu NP, Mahato SB, Sarkar SK, Poddar G (1996) Triterpenoid saponins from *Gymnema sylvestre*. Phytochemistry 41:1181–1185. https://doi.org/10.1016/0031-9422(95)00782-2

Seemann S, Zohles F, Lupp A (2017) Comprehensive comparison of three different animal models for systemic inflammation. J Biomed Sci 24:60. https://doi.org/10.1186/s12929-017-0370-8

Shi L, Kishore R, Mcmullen MR, Nagy LE (2002) Lipopolysaccharide stimulation of ERK1/2 increases TNF-α production via Egr-1. Am J Physiol 282:C1205–C1211. https://doi.org/10.1152/ajpcell.00511.2001

Song KS, Lee WJ, Chung KC, Koo JS, Yang EJ, Choi JY, Yoon JH (2003) Interleukin-1 beta and tumor necrosis factor-alpha induce MUC5AC overexpression through a mechanism involving ERK/p38 mitogen-activated protein kinases-MSK1-CREB activation in human airway epithelial cells. J Biol Chem 278:23243–23250. https://doi.org/10.1074/jbc.M300096200

Spadaro S, Fogagnolo A, Campo G, Zucchetti O, Verri M, Ottaviani I, Tunstall T, Grasso S, Scaramuzzo V, Murgolo F, Marangoni E, Vieceli Dalla Sega F, Fortini F, Pavasini R, Rizzo P, Ferrari R, Papi A, Volta CA, Contoli M (2021) Markers of endothelial and epithelial pulmonary injury in mechanically ventilated COVID-19 ICU patients. Crit Care 25:74. https://doi.org/10.1186/s13054-021-03499-4

Spagnolo P, Balestro E, Aliberti S, Cocconcelli E, Biondini D, Casa GD, Sverzellati N, Maher TM (2020) Pulmonary fibrosis secondary to COVID-19: a call to arms? Lancet Respir Med 8:750–752. https://doi.org/10.1016/s2213-2600(20)30222-8

Steinberg KP, Milberg JA, Martin TR, Maunder RJ, Cockrill BA, Hudson LD (1994) Evolution of bronchoalveolar cell populations in the adult respiratory distress syndrome. Am J Respir Crit Care Med 150:113–122. https://doi.org/10.1164/ajrccm.150.1.8025736

Subramani S K, Gupta Y, Manish M & Prasad G (2020) *Gymnema sylvestre* A—potential inhibitor of COVID-19 main protease by MD simulation study. ChemRxiv. https://doi.org/10.26434/chemrxiv.12333251.v1

Takeuchi O, Akira S (2010) Pattern recognition receptors and inflammation. Cell 140:805–820. https://doi.org/10.1016/j.cell.2010.01.022

Tang Y, Liu J, Zhang D, Xu Z, Ji J, Wen C (2020a) Cytokine storm in COVID-19: the current evidence and treatment strategies. Front Immunol 11:1708–1708. https://doi.org/10.3389/fimmu.2020.01708

Tang Y, Liu J, Zhang D, Xu Z, Ji J, Wen C (2020b) Cytokine storm in COVID-19: the current evidence and treatment strategies. Front Immunol. https://doi.org/10.3389/fimmu.2020.01708

Tirunavalli SK, Gourishetti K, Kotipalli RSS, Kuncha M, Kathirvel M, Kaur R, Jerald MK, Sistla R, Andugulapati SB (2021a) Dehydrozingerone ameliorates Lipopolysaccharide induced acute respiratory distress syndrome by inhibiting cytokine storm, oxidative stress via modulating the MAPK/NF-κB pathway. Phytomedicine 92:153729. https://doi.org/10.1016/j.phymed.2021.153729

Tirunavalli SK, Gourishetti K, Kotipalli RSS, Kuncha M, Kathirvel M, Kaur R, Jerald MK, Sistla R, Andugulapati SB (2021b) Dehydrozingerone ameliorates Lipopolysaccharide induced acute respiratory distress syndrome by inhibiting cytokine storm, oxidative stress via modulating the MAPK/NF-κB pathway. Phytomedicine 92:153729–153729. https://doi.org/10.1016/j.phymed.2021.153729

Tiwari P, Mishra BN, Sangwan NS (2014a) Phytochemical and pharmacological properties of *Gymnema sylvestre*: an important medicinal plant. Biomed Res Int 2014:830285–830285. https://doi.org/10.1155/2014/830285

Tiwari P, Mishra BN, Sangwan NS (2014b) Phytochemical and pharmacological properties of *Gymnema sylvestre*: an important medicinal plant. Biomed Res Int 2014:830285. https://doi.org/10.1155/2014/830285

Tsai Y-F, Yu H-P, Chang W-Y, Liu F-C, Huang Z-C, Hwang T-L (2015) Sirtinol inhibits neutrophil elastase activity and attenuates lipopolysaccharide-mediated acute lung injury in mice. Sci Rep 5:8347. https://doi.org/10.1038/srep08347

Tseng T-L, Chen M-F, Tsai M-J, Hsu Y-H, Chen C-P, Lee TJF (2012) Oroxylin-A rescues LPS-induced acute lung injury via regulation of NF-κB signaling pathway in rodents. PLoS One 7:e47403–e47403. https://doi.org/10.1371/journal.pone.0047403

Turner MD, Nedjai B, Hurst T, Pennington DJ (2014) Cytokines and chemokines: at the crossroads of cell signalling and inflammatory disease. Biochimica Et Biophysica Acta (BBA) 1843:2563–2582. https://doi.org/10.1016/j.bbamcr.2014.05.014

Van Der Bruggen T, Nijenhuis S, Van Raaij E, Verhoef J, Van Asbeck BS (1999) Lipopolysaccharide-induced tumor necrosis factor alpha production by human monocytes involves the raf-1/MEK1-MEK2/ERK1-ERK2 pathway. Infect Immun 67:3824–3829. https://doi.org/10.1128/iai.67.8.3824-3829.1999

Wei J, Chen G, Shi X, Zhou H, Liu M, Chen Y, Feng D, Zhang P, Wu L, Lv X (2018) Nrf2 activation protects against intratracheal LPS induced mouse/murine acute respiratory distress syndrome by regulating macrophage polarization. Biochem Biophys Res Commun 500:790–796. https://doi.org/10.1016/j.bbrc.2018.04.161

Yang S-C, Tsai Y-F, Pan Y-L, Hwang T-L (2021) Understanding the role of neutrophils in acute respiratory distress syndrome. Biomed J 44:439–446. https://doi.org/10.1016/j.bj.2020.09.001

Yoshikawa K, Arihara S, Matsuura K (1991) A new type of antisweet principles occurring in *Gymnema sylvestre*. Tetrahedron Lett 32:789–792. https://doi.org/10.1016/S0040-4039(00)74887-8

Yoshikawa K, Hirai H, Tanaka M, Arihara S (2000) Antisweet natural products. XV. Structures of Jegosaponins A-D from Styrax japonica SIEB. et ZUCC. Chem Pharm Bull 48:1093–1096. https://doi.org/10.1248/cpb.48.1093

Yu J, Wang Y, Li Z, Dong S, Wang D, Gong L, Shi J, Zhang Y, Liu D, Mu R (2016) Effect of heme oxygenase-1 on mitofusin-1 protein in LPS-induced ALI/ARDS in rats. Sci Rep 6:36530. https://doi.org/10.1038/srep36530